THE OXIDATION OF ILMENITE: A KINETIC STUDY

by

Lawrence J. "Corsa," III

Thesis submitted to the Graduate Faculty of the

Virginia Polytechnic Institute and State University

in partial fulfillment of the requirements for the degree of

MASTER OF SCIENCE

in

Materials Engineering

APPROVED:

T. P. Floridis, Chairman

J. L. Lytton

W. R. Hibbard

C. W. Spencer, Dept. Head

June, 1977

Blacksburg, Virginia

ACKNOWLEDGMENTS

The author wishes to express his gratitude to Dr. T. P. Floridis of the Materials Engineering Department of VPI&SU. Dr. Floridis initiated this research and provided funds for my assistantship. Without his technical advice and assistance this thesis would not have been possible.

The author also extends thanks to Drs. J. L. Lytton, C. W. Spencer, and M. R. Louthan, Jr. for their wisdom in times of disaster, and to the other graduate students in the department for their help and friendship.

All X-ray analyses were performed in the facilities of Dr. C. R. Houska. The results obtained were necessary to the research, and the author is grateful for the use of the equipment.

Many other people contributed their patience, advice, and assistance to the successful conclusion of my stay here at VPI&SU. To all these people I sincerely express my thanks and friendship, especially to , who suffered more for this than I.

TABLE OF CONTENTS

Page

ACKNOWLEDGMENTS ii

LIST OF FIGURES iv

LIST OF TABLES. vi

INTRODUCTION. 1

REVIEW OF LITERATURE. 3

The System Fe-Ti-O 3
Ilmenite and its Oxidation Products. 5
Kinetic Methods and the Oxidation of Ilmenite. 10

EXPERIMENTAL PROCEDURES 12

Oxidation Study. 15
Product Determination. 15
Oxidation Kinetics 16

RESULTS AND DISCUSSION. 19

The Oxidation Products of Ilmenite 19
The Kinetics of Ilmenite Oxidation 29

CONCLUSIONS 65

RECOMMENDATIONS FOR FURTHER STUDY 67

BIBLIOGRAPHY. 68

VITA. 71

ABSTRACT

LIST OF FIGURES

Figure		Page
1.	The system $FeO-Fe_2O_3-TiO_2$ showing the three solid solution series. At low temperatures the join $TiO_2-Fe_3O_4$ becomes stable.	4
2.	The system $FeO-TiO_2$ at oxygen pressures defined by the iron-wüstite equilibrium	6
3.	The system Fe-Ti-O showing $Fe_2O_3-TiO_2$ and $FeO-TiO_2$ binary joins	7
4.	The equipment used in the thermogravimetric analysis	17
5a.	Ilmenite as synthesized (-325 mesh) 500X	25
5b.	Ilmenite as synthesized (-325 mesh) 2000X.	26
5c.	Ilmenite oxidized 24 hours at 520°C (-325 mesh).	27
5d.	Ilmenite oxidized 24 hours at 790°C (-325 mesh).	28
6.	The percentage of theoretical oxidation versus time for the 45-75 μm particles	46
7.	The percentage of theoretical oxidation versus time for 75-150 μm particles.	47
8.	The percentage of theoretical oxidation versus time for 150-180 μm particles	48
9.	A plot of temperature versus time for the kinetic samples.	51
10.	The percentage of theoretical oxidation versus time for all three particle fractions as determined from a 'piecewise' least squares technique.	54
11.	A plot of oxidation rate ($\log_{10}$d(% ox)/dt) versus reciprocal absolute temperature.	57
12.	A plot of oxidation rate (normalized to interfacial area) versus reciprocal absolute temperature	58

Figure Page

13. A plot of oxidation rate (normalized to product layer thickness squared) versus reciprocal absolute temperature. 59

LIST OF TABLES

Table		Page
I.	Analysis of Reagents	13
II.	The Interplanar Spacings Obtained Experimentally From -325 Mesh Synthetic Ilmenite	20
III.	The Interplanar Spacings of Ilmenite and Its Reported Oxidation Products	21
IV.	Experimental Results for Samples	30
V.	Weight Gained	50
VI.	Calculated Results for the Oxidation of Particles	60
VII.	Calculated Resulted Used in Determination of Activation Energies by the Method of Linear Regression	64

INTRODUCTION

Titanium is rapidly finding use as a non-aviation construction material largely on the merits of its excellent mechanical properties. No metal since aluminum has found such a wide variety of applications so soon after its commercial introduction. Unlike aluminum, no economical process for the industrial manufacture of titanium metal has been discovered. This prevents titanium from being used in many products which could benefit from its use and keeps it in the category of an exotic material. For these reasons, a cheaper, more efficient method of winning titanium from its natural state is of large concern to the industry.

The two minerals most commonly processed for their titanium content are rutile (TiO_2) and ilmenite ($FeTiO_3$). Of these, ilmenite is by far the cheapest and most abundant material[1] but is less desirable from the standpoint of processing. To date, industry has used ilmenite mostly for the production of pigment grade rutile, but as the reserves of rutile ores have become less readily available, the gradual substitution of ilmenite ores has increased[2].

The major processes currently used for processing ilmenite are[1]:

(a) Smelting with coal or coke in an electric furnace to produce molten iron and a titanium-rich slag (the Sorel slag process)

(b) A selective chlorination using hydrochloric acid or a combination of chlorine and carbon monoxide gases at high temperatures and pressures

(c) Sulphidization using either sulfuric acid, hydrogen sulfide with carbon, or sulfur vapor at high temperatures and pressures.

(d) Solid state reduction of the iron oxide component in the presence of a catalyst (the Becher process).

These processes end with a concentrate high in TiO_2, which is then processed for titanium metal. Only the Becher and Sorel slag methods have been used on an industrial scale.

The direct treatment of ilmenite for the extraction of titanium is considered desirable, but an economical process has not been developed. Direct reduction processes are quite sluggish[3,4], although prior oxidation treatment holds much promise for the future[4,5,6]. In order to optimize this type of process, a thorough study of the oxidation process in ilmenite is of primary importance. The thrust of the present investigation will be to determine the kinetics of the oxidation process and the end products of roasting.

REVIEW OF LITERATURE

Previous work pertinent to this investigation falls into three basic categories:

(1) Studies of the equilibrium system iron-titanium-oxygen and its subsystems

(2) Studies of the mineral ilmenite and its alteration products

(3) Analytical methods for the determination of kinetic data using non-isothermal techniques.

The System Fe-Ti-O

Much of the thermodynamic and equilibrium data available in the literature were determined for the pseudo-ternary system 'FeO'-Fe_2O_3-TiO_2 at temperatures above 900°C[7,8,9]. This system has been shown[10] to have three solid solution series in this range of temperatures (see Figure 1):

(1) The cubic system magnetite-ulvospinel (Fe_3O_4-Fe_2TiO_4) series

(2) The rhombohedral hematite-ilmenite (Fe_2O_3-$FeTiO_3$) series

(3) The spinel pseudobrookite (Fe_2TiO_5-$FeTi_2O_5$) series.

A fourth solid solution series, magnetite-rutile (Fe_3O_4-TiO_2) is found at temperatures below 400°C[11]. The pseudobinary join Fe_2TiO_5-$FeTi_2O_5$ was first shown to be a complete solid solution series above 1150°C by Akimoto, Nagata, and Katsura[12] and has since been confirmed[7,13]. $FeTi_2O_5$ is an unnamed compound not found in nature. The join Fe_2O_3-$FeTiO_3$ exhibits solid solution above 950°C, and the join Fe_3O_4-Fe_2TiO_4 is a complete solid solution series at temperatures as low as 600°C[14].

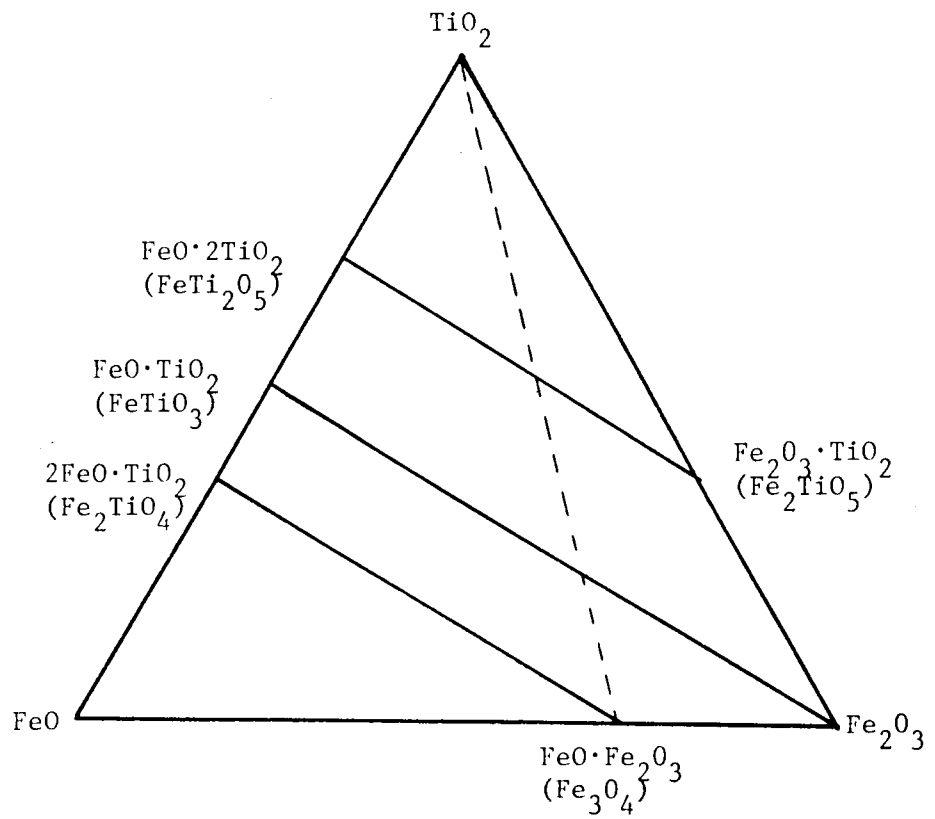

Figure 1. The system $FeO-Fe_2O_3-TiO_2$ showing the three solid solution series. At low temperatures the join $TiO_2-Fe_3O_4$ becomes stable. (From Lindsley[11])

The join $FeO-TiO_2$ (Figure 2) of the Fe-Ti-O system (Figure 3) is of major importance to this study since ilmenite is but one of three compounds in this binary system. Each of these compounds is an end member of a solid solution series in the Fe_2O_3-'FeO'-TiO_2 system. An early study[15] revealed only the compounds ulvospinel ($2FeO \cdot TiO_2$) and ilmenite ($FeO \cdot TiO_2$), but more recent research[12,16] demonstrated the existence of $FeO \cdot 2TiO_2$.

Ilmenite and its Oxidation Products

There is much apparent disagreement in the literature concerning the behavior of ilmenite at temperatures below 1000°C, as pointed out by Rao and Rigaud[17]. Much of this is traceable to a fundamental difference in the samples used. Experiments involving the oxidation products of ilmenite are performed for either mineralogical or metallurgical reasons, with the former preferring to use naturally obtained ilmenite concentrates. Temple[18] has investigated several of the commercially available ilmenite ores and found that they were not ilmenite ('FeO' content 48%), but 'altered' ilmenite, or leucoxene, with 'FeO' contents ranging from 0.1% to 49%. He speculated that this alteration took place by slowly progressing oxidation and leaching of the iron compounds. In any case, it cannot be expected that these materials would behave like chemically pure $FeTiO_3$.

Recent investigations involving synthetic or hand-picked grains of natural ilmenite report the following groups of reactions:

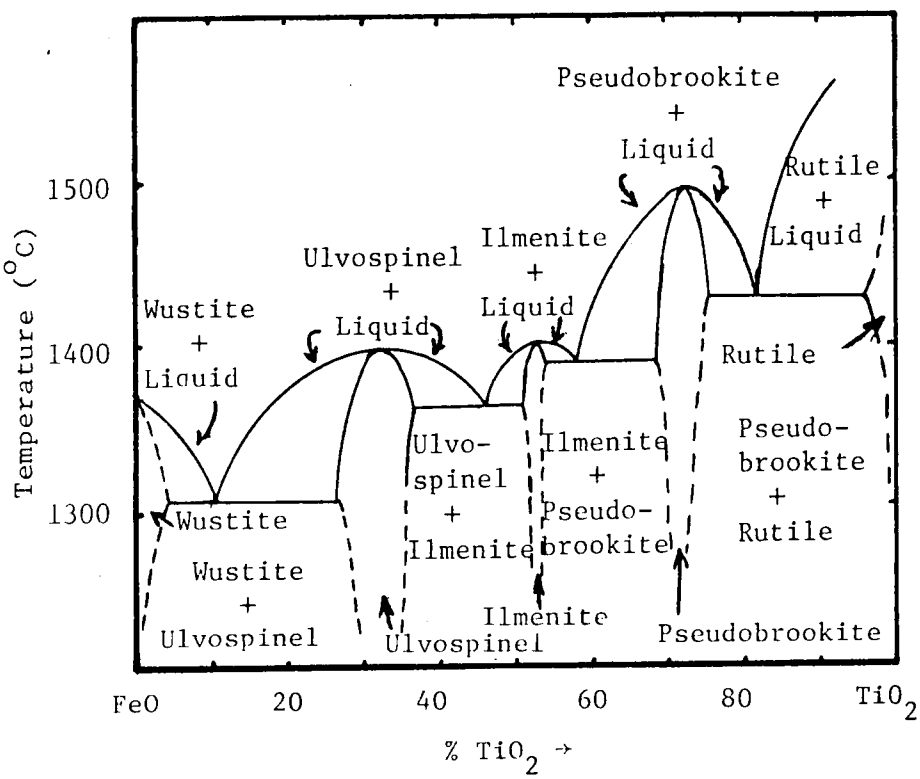

Figure 2. The system FeO-TiO_2 at oxygen pressures defined by the iron-wüstite equilibrium. (From MacChesney and Muan[16])

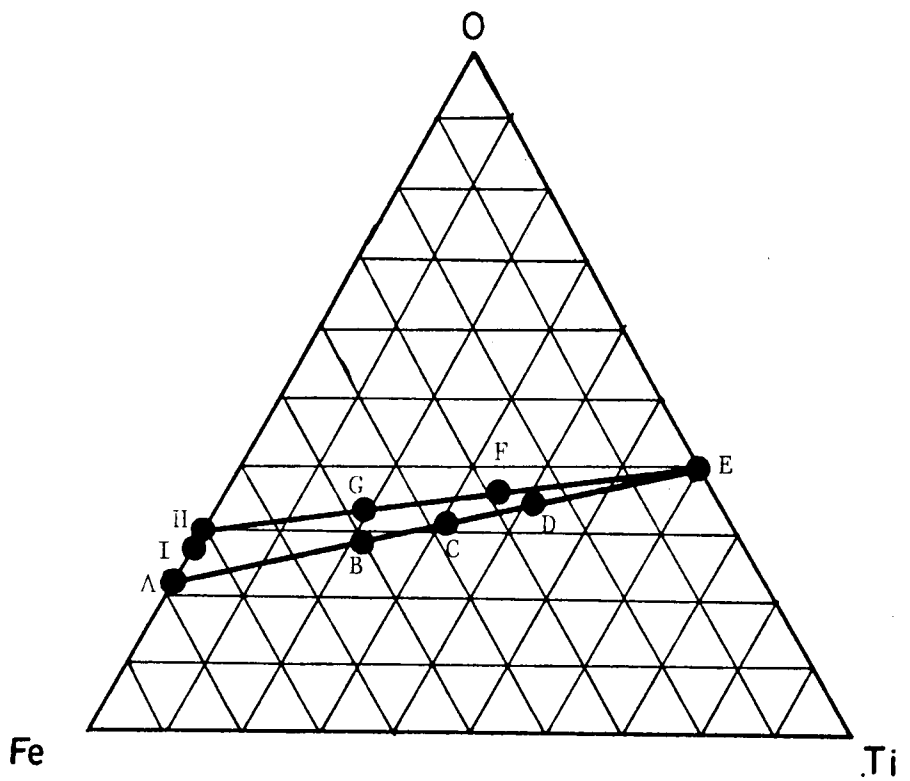

A - FeO
B - Fe_2TiO_4
C - $FeTiO_3$
D - $FeTi_2O_5$
E - TiO_2
F - $Fe_2Ti_3O_9$
G - Fe_2TiO_5
H - Fe_2O_3
I - Fe_3O_4

Figure 3. The system Fe-Ti-O showing Fe_2O_3-TiO_2 and FeO-TiO_2 binary joins.

(1) as suggested by Rao and Rigaud[17,19]

(a) below 770°C, hematite and rutile form

$$4FeTiO_3 + O_2 \rightarrow 2Fe_2O_3 + 4TiO_2$$

(b) from 770°C to 890°C, pseudorutile and hematite form

$$12FeTiO_3 + 3O_2 \rightarrow 4Fe_2Ti_3O_9 + 2Fe_2O_3$$

(c) above 890°C, pseudobrookite and rutile form

$$4FeTiO_3 + O_2 \rightarrow 2Fe_2TiO_5 + 2TiO_2$$

(2) as suggested by Grey and Reid[20], Ramdohr[21], Curnow and Parry[22], Teufer and Temple[23], and Overholt, Vaux, and Rodda[24]

(a) below 800°C, pseudorutile and hematite form

(b) above 800°C, pseudobrookite and rutile form

(3) as suggested by Karkhanavala and Momin[25]

(a) at 650°C, pseudobrookite and rutile, 'probably' with small amounts of hematite

(b) at 850°C, a 1:5:7 molar mixture of hematite, pseudobrookite and rutile

$$12FeTiO_3 + 3O_2 \rightarrow Fe_2O_3 + 5Fe_2TiO_5 + 7TiO_2$$

Teufer and Temple[23] further demonstrated that pseudorutile decomposes above 800°C to form pseudobrookite and rutile by the reaction:

$$Fe_2Ti_3O_9 \rightarrow Fe_2TiO_5 + 2TiO_2$$

and demonstrated the orientational relationships of an oxidized single crystal to be

Ilmenite	Pseudorutile	Rutile
$\{0001\}[11\bar{2}0]$	$\|\|\{0001\}[10\bar{1}0]$	$\|\|\{010\}[001]$

The mineral pseudorutile has never been synthesized from its constituent compounds, hematite and rutile[19]. Larrett and Spencer (see ref. 17, p. 325) report that pseudorutile only occurred when synthetic ilmenite was oxidized, but all agree that pseudorutile is a phase distinct from both the dubious $Fe_2O_3 \cdot 3TiO_2$ compound 'Arizonite' discovered by Palmer[26] and the mixture reported by Karkhanavala and Momin[25]. (It was pointed out by Temple[18] that the unidentifiable peaks reported by Karkhanavala and Momin obtained from the oxidation products at 650°C and 850°C are clearly due to the formation of pseudorutile, a compound not identified in 1959.) The inability to synthesize pseudorutile directly is believed due to either the metastable nature of the compound and the corresponding need for a specific reaction path with divalent iron as the diffusing specie[20] or to the slowness of the diffusion process in the temperature range where pseudorutile exists[17].

The compound Fe_2TiO_5 was shown by Pauling (see ref. 12, p. 38 and ref. 20, p. 188) to have the orthorhombic pseudobrookite structure. It is an unstable compound with a lower temperature limit between 800 and 900°C. Rao and Rigaud[17] determined pseudobrookite to be unstable with respect to pseudorutile at temperatures below about 900°C using differential thermal and gravimetric analysis, while others[20-24] have reported the presence of pseudobrookite as low as 800°C by actual experiment.

Kinetic Methods and the Oxidation of Ilmenite

The only investigations of the kinetics of the oxidation of ilmenite reported in the literature are those of Rao and Rigaud[19] and Karkhanavala and Momin[25], with the results of the former being central to this thesis. The latter investigation amounted to a single published thermogram obtained under conditions of linear temperature increase. The principle features of this thermogram were:

(1) small amounts of oxidation at temperatures below 300°C

(2) a sharp increase in the reaction rate above 500°C

(3) a failure of the reaction to reach its theoretical limit of 5.2% weight gain .

There was no 'abrupt weight gain above 800°C' as reported by Rao and Rigaud in their study. Karkhanavala and Momin maintained temperature at 850°C to allow the reaction to go to completion. This appeared on their chart of weight gain versus temperature as a vertical line, which was apparently mistaken for a sharp weight increase.

Rao and Rigaud were more thorough in their experimental work. Using both isothermal and non-isothermal techniques, they determined that ilmenite powders oxidized according to the logarithmic rate law with an activation energy of 9.5 kcal/mole in dry oxygen. They also determined that ilmenite platelets oxidized parabolically with an activation energy of 20 kcal/mole up to 800°C, and 43 kcal/mole above 800°C. The morphology of the product layer was studied using both a scanning electron microscope equipped with an energy-dispersive

analysis unit for determining the distribution of elements and platinum markers imbedded in the platelets. They report that oxygen diffusion through the product layer is the rate limiting step at temperatures lower than 900°C.

For this investigation, non-isothermal techniques were employed in order to obtain large amounts of information from a small number of samples. A short discussion of the technique is given by Kubaschewski and Hopkins[26] and by Wood[27], both of whom mention that the temperature must increase linearly with time. This condition was required to make a mathematic variable transformation, which was not shown to be necessary in the general treatment of Freeman and Carroll[28]. Using thermogravimetric analysis even without linear heating rates, good agreement with isothermal data has been observed[29-31]. A major problem with this method is that the reaction mechanism must be determined by trial and error, with the rate law determined from the most appropriate model[32,33].

EXPERIMENTAL PROCEDURES

The techniques and equipment used in the course of this study are presented in the following sections. All additional information necessary to the reproduction of these data are also included.

Sample Preparation

The ilmenite ($FeTiO_3$) required for these experiments was synthesized using commercially available reagents using the following procedure:

(a) Iron oxide (Fe_2O_3), as hematite powder, and titanium dioxide (TiO_2), as anatase powder (see Table I), were dried for several days at 125°C to reduce the inaccuracies that could be caused by moisture in the reagents.

(b) The powders were weighed on the Sartorius type 2842 analytical balance which was capable of one-tenth of a milligram precision. Twenty-five grams of mixture were prepared in the exact stoichiometric proportions for the reaction

$$2Fe_2O_3 + 4TiO_2 = 4FeTiO_3 + O_2$$

(c) The powders were blended overnight under acetone and air-dried. The mixture was ground with a mullite mortar and pestle to achieve a finer, more homogeneous mixture.

(d) The material was packed into a four-inch quartz combustion boat and placed in the uniform temperature zone of a Lindberg 'Hevi-Duty' furnace. The furnace was equipped with a mullite

TABLE I. Analysis of Reagents

Titanium Dioxide (TiO_2, as anhydrous anatase) 99.95% pure obtained from J. T. Baker Chemical Co.

Water Soluble Salts	0.03%
Arsenic (As)	0.0001%
Iron (Fe)	0.002%
Lead (Pb)	0.006%
Zinc (Zn)	0.009%

Ferric Oxide (Fe_2O_3, as red, anhydrous hematite) 99.81% pure obtained from the Fisher Scientific Company.

Arsenic (As)	0.002%
Nitrate (NO_3)	0.01%
Phosphate (PO_4)	0.02%
Sulfate (SO_4)	0.05%
Manganese (Mn)	0.05%
Copper (Cu)	0.009%
Substances not p'ptd by NH_4OH	0.04%
Zinc (Zn)	0.007%

furnace tube and a Lindberg controller. The temperature was measured with a chromel-alumel thermocouple and a potentiometer. The system was flushed with carbon dioxide gas flowing at 300 cc/min for at least one hour prior to the start of the run. The flow rate was then decreased to 180 cc/min. As the temperature increased, a 90% argon-10% hydrogen mixture was added to the gas stream. The gas mixture was chosen so that, at 1000°C, the following reactions would be occurring:

(1) the reduction of hematite to "wüstite"[34]

$$Fe_2O_3 + CO \rightarrow 2'FeO' + CO_2$$

$$Fe_2O_3 + H_2 \rightarrow 2'FeO' + H_2O$$

(2) the "water-gas" equilibrium[35]:

$$CO_2 + H_2 = CO + H_2O$$

Titanium dioxide does not participate in the solid-fluid equilibrium. Six days were allowed for the solid state reaction

$$'FeO' + TiO_2 \rightarrow FeTiO_3$$

to occur.

(e) The furnace was opened and the sample quickly removed at 24 hour intervals for the first four days. The sintered material was broken and crushed with a steel impact mortar and replaced in the furnace. This procedure prevented the sintering process from hindering the gas infiltration, and further reduced the chance of inhomogeneity in the material.

The material was left undisturbed for the final 48 hours to allow sintering to consolidate the fine powders.

(f) The ilmenite was sampled and examined with X-rays to assure that the desired reaction had gone to completion. Finally, the mineral was crushed and sieved to obtain three particle size fractions. The finest particles (-325 mesh) were used in the X-ray identifications.

Oxidation Study

The experiment was separated into two areas:

(a) the determination of the oxidation products and morphology

(b) the study of the rates of oxidation.

Product Determination

Five-gram samples of synthetic ilmenite were returned to the same Lindberg furnace used in the synthesis of the material. The specimens were held under flowing dry oxygen at temperatures in the range 500°C - 850°C for periods of 12 to 24 hours. The oxidized samples were air-quenched and subjected to an X-ray diffraction analysis. The Siemens diffractometer was equipped with a graphite crystal monochromator to filter the K_β component of the copper K radiation. The sample was held in a device which tumbled and oscillated the loose powder specimens to prevent any effects of preferred powder orientation. The scans were performed at ½ or 1 degree/minute under 50 kV radiation. A scintillation detector was

used for maximum sensitivity to the weak diffracted intensities produced.

Oxidation Kinetics

Powdered ilmenite specimens weighing from 300 to 400 mg were loosely placed in a quartz crucible. A range of sample weights was used in place of a single weight to determine if the height of material in the crucible had an effect on the course of oxidation. For example, if the particles were sintering as the temperature was increasing, the sample height might eventually affect the path length for the penetration of oxygen to the bottom of the crucible.

An Ainsworth Recording Balance system, type RV-AU-2, continuously monitored the weight and temperatures of the specimen. The system employed a Lindberg 'Hevi-Duty' furnace mounted vertically beneath the left pan of the balance (see Figure 4). The final temperature of the run was preset on a Honeywell type 54261 controller whose thermocouple was placed in the furnace insulation at the level of the hot zone.

The sample was placed in a platinum basket which was suspended from the left pan by a platinum wire. The temperature of the specimen was monitored by a sheathed chromel-alumel thermocouple located 7 mm below the sample, well within the 4 cm uniform temperature zone of the furnace.

The entire system, including the balance enclosure, was flushed with dry oxygen for at least thirty minutes before each run. The

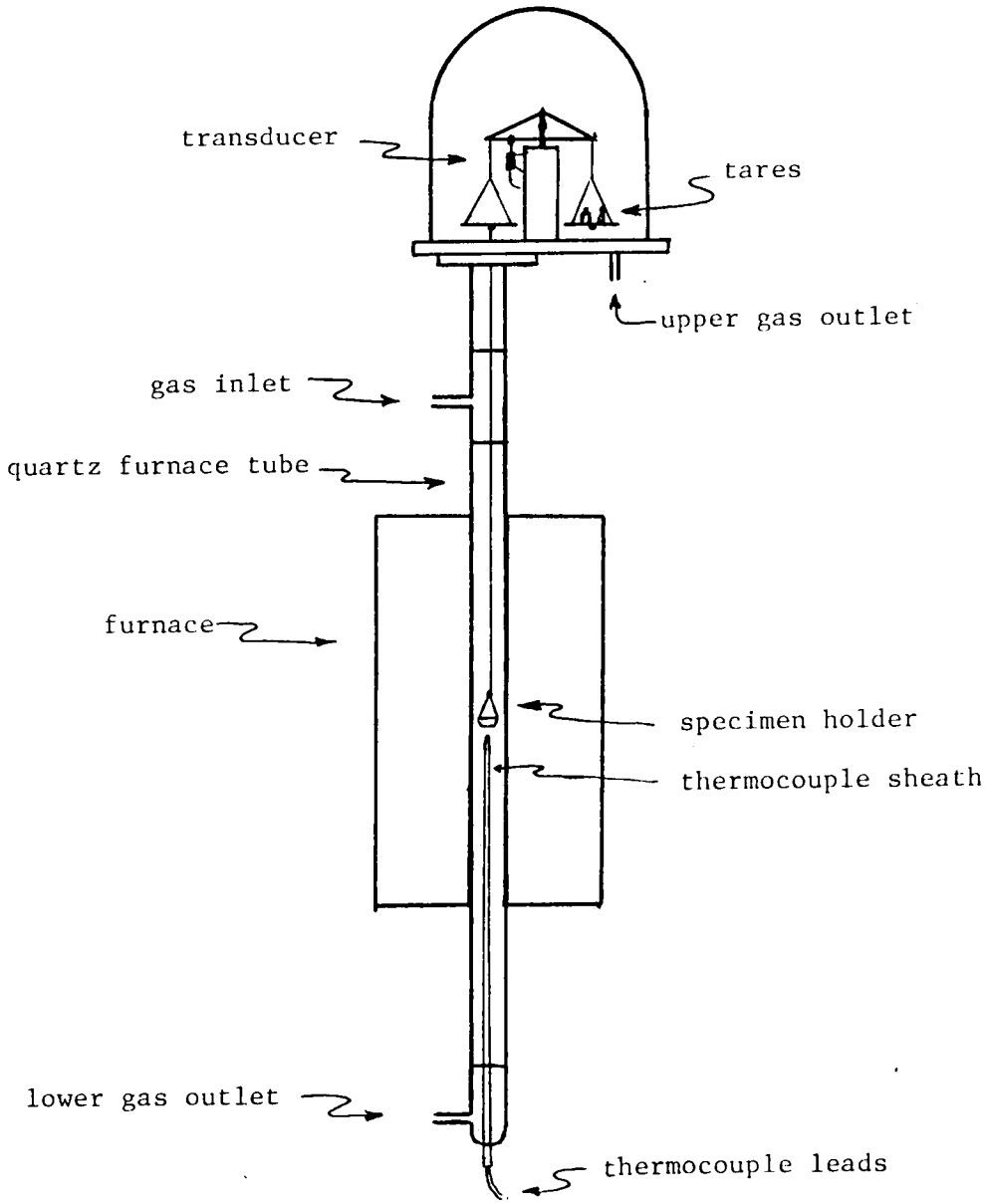

Figure 4. The equipment used in the thermogravimetric analysis.

electronics were allowed to equilibrate during this time. The flow rate was reduced to 200 cc/min and the balance enclosure gas outlet was closed at least two minutes prior to the application of power to the furnace windings. No change in sample weight was detected during this period.

The experiment commenced when power was applied to the furnace winding. A Variac, rather than a switch, was used to prevent sudden changes in line voltage which could affect the equipment. The high inertia furnace was allowed to heat at its own rate, which varied continuously from 35°C/min to less than 10°C/min as the experiment progressed. Data were taken at 25°C intervals from 300°C to 850°C, at which time the experiment was terminated. Each run required 50 to 55 minutes from start to finish, depending upon ambient temperature.

This procedure was repeated for five runs each of three particle size fractions. Four standardizing runs were also made to compensate for convection current and bouyancy effects encountered as the gas passed down through the hot zone of the furnace. Titanium dioxide, which had been dried and vacuum degassed, was chosen as the standard material since it is inert under oxidizing conditions over the temperature range of interest. The weight of all standards was checked with the analytical balance before and after each run with no change noted. The weight increase of each sample was also checked and only small discrepancies were noted. These could be due to additional oxidation taking place during the six hour period required to cool the furnace.

RESULTS AND DISCUSSION

The results of this study are best presented in two parts for the purpose of discussion:

(1) the determination of the oxidation products

(2) the determination of kinetic data for the oxidation reaction. The results will be correlated in the next section.

The Oxidation Products of Ilmenite

X-ray diffraction analysis was performed as previously described to determine the phases present at the various temperatures. The results of this work are collected in Table II. Table III is provided for purposes of comparison and contains the interplanar spacings of the reported oxidation products obtained by some previous investigations. It must be remembered that the diffracted intensity from these specimens is quite small due to the very fine-grained nature of the oxidation products. This tends to make the material very amorphous in character, causing the X-ray peaks to generally be broad and diffuse[18,36]. As a consequence of this, no accuracy better than $\pm$ 0.02Å is claimed for the experimentally determined lattice spacings. No intensity data are reported because no reliable data could be obtained from the X-ray charts.

The synthetic ilmenite had no discernable peaks due to the presence of impurities, unreacted material, or other iron-titanium compounds. Magnetite and ulvospinel have occasionally been found by other investigators[17] and in previous synthesis attempts by

TABLE II. The Interplanar Spacings Obtained Experimentally From -325 Mesh Synthetic Ilmenite.

Sample IL3-1 as synthesized	Sample IL3-2 oxidized 24 hours 520°C	Sample IL3-3 oxidized 24 hours 615°C	Sample IL3-4 oxidized 24 hours 710°C	Sample IL3-5 oxidized 24 hours 790°C	Sample IL3-6 oxidized 12 hours 850°C
	2.89	2.89			
			2.88	2.88	2.86
2.74	2.74		2.74	2.74	2.73
		2.73			
		2.70	2.70	2.70	2.68
2.54	2.53				
		2.52	2.52	2.52	
			2.50		2.50
					2.47
	2.43	2.44	2.43	2.43	2.44
2.24	2.23				
		2.20	2.20	2.20	2.21
				2.11	2.19
			2.10		
1.87	1.87				1.96
		1.84	1.84	1.84	1.85
1.73	1.73				1.74
		1.71			1.71
			1.70	1.70	
			1.69		1.69
			1.67	1.67	
1.64	1.64	1.64	1.64	1.64	1.66
					1.63
			1.60		1.61
					1.53
1.50	1.50				DB* (1.50 1.48)
1.47	1.47		1.49		
		1.48		1.48	
		1.45	1.45	1.45	DB 1.45
		1.43	1.43	1.43	
		1.37	1.37	1.37	DB 1.42
					DB (1.36 1.34)
1.34	1.34				

*Diffuse Band

TABLE III. The Interplanar Spacings of Ilmenite and Its Reported Oxidation Products.

Hematite (Fe_2O_3)	Ilmenite ($FeTiO_3$)	Rutile (TiO_2)	Anatase (TiO_2)	Pseudobrookite (Fe_2TiO_5)	Pseudorutile ($Fe_2Ti_3O_9$)
ASTM No. 13-0534	ASTM No. 3-0781	ASTM No. 21-1276	ASTM No. 4-0477	ASTM No. 9-0182	From Grey & Reid[20]
					2.88
	2.74			2.75	2.74
2.69					
	2.54				
2.51					2.50
		2.49		2.45	
			2.43		2.43
			2.38		
			2.34		
					2.31
	2.23	2.30		2.22	
2.20				2.20	2.20
		2.19			
					2.12
2.07					
		2.05			2.01
				1.97	
			1.89	1.86	
	1.86				
1.84				1.74	
	1.72				
			1.70		1.71
1.69		1.69			
			1.66	1.66	1.67
1.63	1.63		1.63	1.63	1.64
1.60		1.62			
				1.54	
	1.50				1.51
			1.49	1.49	1.49
1.48		1.48	1.48		
1.45	1.47	1.45			
		1.42		1.42	1.43
			1.37	1.37	
		1.36			
1.35					
	1.34				
1.31				1.31	

the author. A crude chemical analysis was accomplished using energy dispersive analysis while the specimen was being examined in the scanning electron microscope. Roughly equal amounts of elemental iron and titanium were present at all points along the several grains tested.

The lines obtained from the sample oxidized for 24 hours at 520°C are still predominantly those of ilmenite, but some new lines have appeared with "d" spacings of 2.20Å, 2.43Å, and 2.89Å. The line at 2.43Å could be attributed to anatase, and the 2.20Å line could be hematite, but all three taken together indicate the presence of pseudorutile. The absence of lines of 2.12Å, 2.01Å, 1.70Å and 1.67Å makes positive identification complicated, but no other reported iron-titanium compound has a lattice reflection at d = 2.89Å.

The sample oxidized at 615°C for one day displayed some lines due to hematite, and some due to the presence of either unreacted ilmenite or increased amounts of pseudorutile. As before, there are lines missing from the pattern of pseudorutile, but there are also lines missing from the patterns of the other possible mineral patterns. At 710°C, the pattern obtained from the oxidation products is certainly that of pseudorutile and hematite. The line at 2.89Å has been gaining steadily in intensity as the temperature was increased, and the lines have become sharper, particularly the low angle lines (large "d" spacing).

The lines due to pseudorutile and hematite are present in the X-ray pattern of the specimen oxidized at 790°C, and generally all the lines present have become sharper and more intense. The disappearance of the lines at 2.50Å and 1.60Å are exceptions to this rule, as is the reappearance of the (019) pseudorutile reflection.

The sample examined at 850°C was reacted only twelve hours as Karkhanavala and Momin[24] had reported that no changes occurred in their diffraction patterns after six hours at this temperature. However, the pattern obtained by this investigator was considerably more amorphous in character than the other patterns. Few of the lines were either intense or sharp. Several diffuse intensity bands were noted. These can be attributed to either several small peaks overlapping or to the presence of solid solution. This discrepancy could be due in part to the increased thickness of the plastic material used to contain the loose powder while the X-ray analysis proceeded. The accuracy obtained from this determination is correspondingly less than from those patterns taken at lower temperatures. However, the presence or absence of intensity was still detectable. Pseudorutile was present in this sample, as shown by the low angle lines, but the phases pseudobrookite and rutile also appeared at this temperature. Clearly all three phases cannot coexist in equilibrium, but there is no reason to expect that equilibrium was reached by the reaction.

In summary, the following has been demonstrated:

(a) at temperatures as low as 520°C, the mineral pseudorutile may be present. The reaction is probably quite sluggish

at this low temperature, indicating that perhaps as much as a month may be required to attain equilibrium.

(b) at 615°C, hematite is clearly present. Lines due to either ilmenite and rutile or, more probably, to pseudorutile are quite sharp.

(c) at 710°C and 790°C pseudorutile and hematite are the only phases present.

(d) at 850°C, pseudorutile is present to some degree, but hematite is no longer detected. Instead, pseudobrookite and rutile have appeared.

The results of the X-ray study indicate general agreement with reported phases. The following conclusions may be drawn:

(1) no lower temperature limit exists at 770°C for the formation of pseudorutile, as reported by Rao and Rigaud[17]. Both this investigation and those of Temple[18] and Karkhanavala and Momin[25] show the occurrence of this mineral at temperatures well below 800°C.

(2) Pseudobrookite occurs at temperatures below 890°C. This again conflicts with Rao and Rigaud, but agrees with Grey and Reid[20] who reported it at 800°C.

The morphology of the ilmenite and its oxidation products can be seen in Figures 5a-d. It must be noted that the microscopy was performed on -325 mesh particles, including fragments and other fines. The fines adhere to the particles making them appear more jagged and

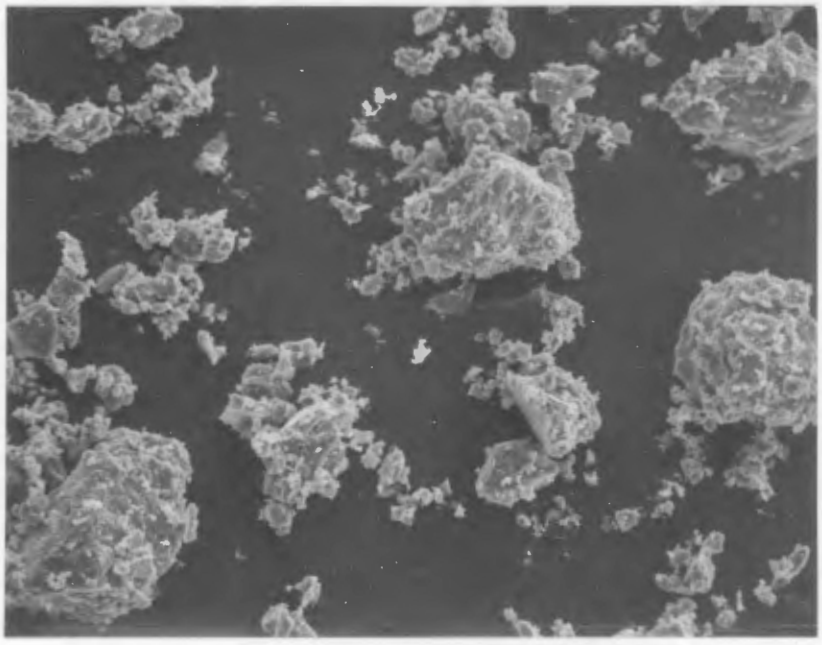

Figure 5a. Ilmenite as synthesized (-325 mesh) 500X.

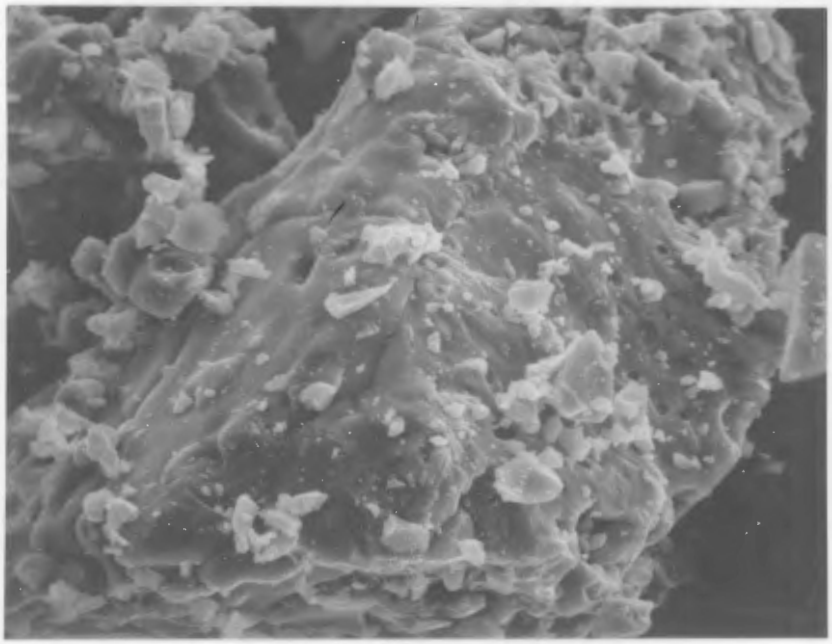

Figure 5b. Ilmenite as synthesized (-325 mesh) 2000X.

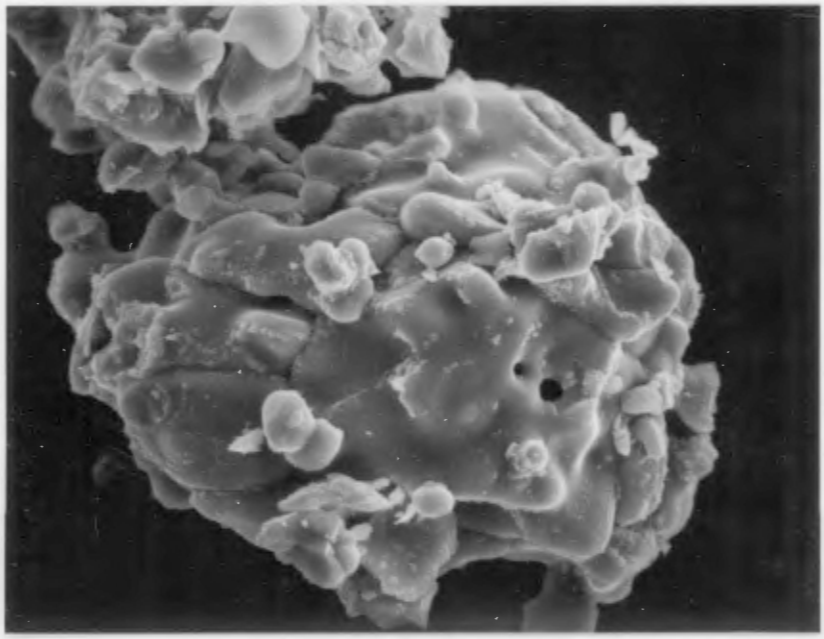

Figure 5c. Ilmenite oxidized 24 hours at 520^{o}C (-325 mesh) 2000X.

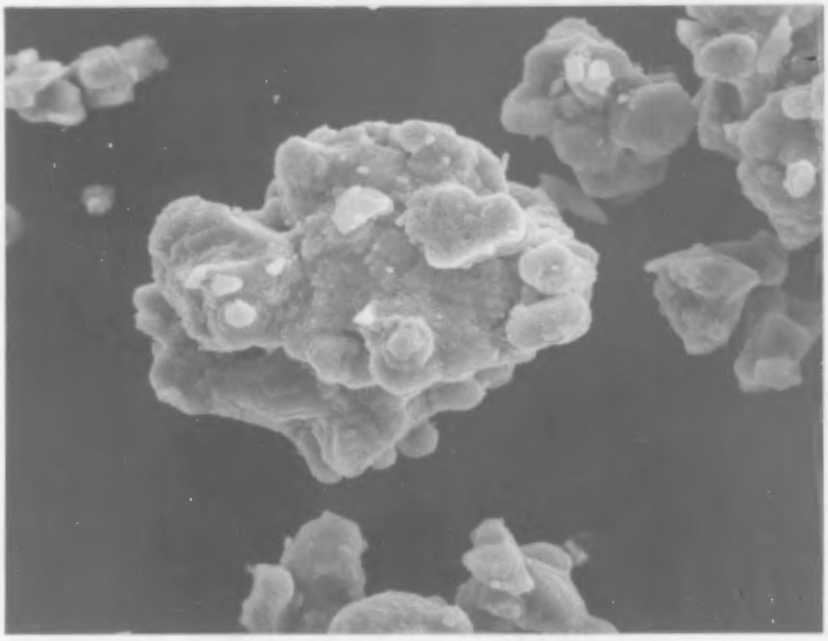

Figure 5d. Ilmenite oxidized 24 hours at 790°C (-325 mesh) 2000X.

broken than they actually are. They would also hide the appearance of a fragmented oxide layer, if one exists.

As synthesized, the particles are generally rounded in shape with an uneven surface. No cracks in the surface are apparent even at higher magnification. After oxidation at 520°C, the surface features are "softer" in appearance and there are no signs of surface fracture. Ilmenite oxidized for 24 hours at 790°C did show signs of high stresses. The surface appears mottled and jagged, and cracking is apparent. The product morphology is important in a study of the kinetic behavior of any material[17] as it may determine the mechanism that controls reaction rate.

The Kinetics of Ilmenite Oxidation

The results of the thermogravimetric analysis of each sample are given in Tables 4a-o and are shown graphically in Figures 6a-c. Although there is some scatter in the data, a definite trend is clearly shown. The scatter is due to improper standardization of the equipment. This source of error can be explained by describing the results of the standardization runs.

Each titanium dioxide standard was performed as if it were an experimental run. The same experimental procedure was followed for all runs, but the standards did not give repeatable results over the initial stage of the experiment. Their apparent weight gain always peaked shortly after power was applied to the furnace, passed through zero and then stabilized at some value. All this occurred

TABLE IVa. Experimental Results for Sample IL4 5-10-2

Temp. (°C)	Time (Sec.)	Weight Gain ($gm \times 10^4$)	Extent of Oxidation (Percent)
300	670	4.1	2.24
325	715	4.8	2.58
350	761	5.6	3.03
375	816	6.3	3.40
400	871	6.8	3.69
425	931	6.9	3.74
450	998	7.3	3.97
475	1073	7.7	4.19
500	1150	8.2	4.44
525	1231	9.2	4.97
550	1318	10.6	5.74
575	1414	12.0	6.52
600	1522	13.8	7.50
625	1639	16.8	9.12
650	1762	19.3	10.59
675	1891	25.2	13.64
700	2038	35.1	19.02
725	2191	47.9	25.98
750	2357	62.9	34.11
775	2542	80.1	43.41
800	2738	98.3	53.28
825	2969	121.1	65.61
850	3240	147.1	79.70

TABLE IVb. Experimental Results for Sample IL4 4-22-2

Temp. (°C)	Time (Sec.)	Weight Gain ($gm \times 10^4$)	Extent of Oxidation (Percent)
300	650	4.6	2.93
325	694	5.5	3.46
350	739	6.2	3.92
375	790	6.7	4.22
400	842	7.1	4.49
425	881	7.3	4.62
450	967	7.6	4.83
475	1042	7.9	5.02
500	1118	8.6	5.44
525	1202	9.5	5.99
550	1291	10.8	6.83
575	1387	12.3	7.80
600	1495	14.2	9.00
625	1615	17.1	10.83
650	1730	21.1	13.36
675	1860	27.5	17.37
700	2002	36.9	23.33
725	2150	47.8	30.24
750	2328	61.5	38.91
775	2530	73.7	46.60
800	2717	87.5	55.33
825	2958	107.5	67.95
850	3185	127.7	80.72

TABLE IVc. Experimental Results for Sample IL4 4-22-1

Temp. (°C)	Time (Sec.)	Weight Gain ($gm \times 10^4$)	Extent of Oxidation (Percent)
300	646	6.0	3.27
325	689	7.2	3.88
350	735	7.0	3.79
375	787	7.3	3.94
400	838	7.6	4.12
425	898	8.0	4.34
450	960	8.4	4.57
475	1035	9.0	4.90
500	1114	9.6	5.20
525	1190	10.5	5.67
550	1282	11.6	6.29
575	1385	13.3	7.23
600	1486	15.4	8.36
625	1598	18.4	9.99
650	1718	23.1	12.54
675	1853	30.0	16.24
700	1992	38.3	20.76
725	2143	49.1	26.63
750	2304	63.2	34.27
775	2486	78.8	42.71
800	2693	96.6	52.35
825	2913	118.4	64.15
850	3158	141.1	76.45

TABLE IVd. Experimental Results for Sample IL4 2-10-1

Temp. (°C)	Time (Sec.)	Weight Gain ($gm \times 10^4$)	Extent of Oxidation (Percent)
300	672	5.3	3.37
325	715	5.9	3.71
350	762	6.6	4.17
375	813	7.3	4.59
400	867	7.8	4.93
425	924	8.2	5.18
450	989	8.5	5.39
475	1057	9.1	5.77
500	1133	9.4	5.94
525	1215	10.7	6.74
550	1304	11.7	7.39
575	1401	12.8	8.11
600	1503	14.7	9.31
625	1615	17.4	11.02
650	1735	21.6	13.67
675	1869	28.9	18.24
700	2011	40.1	25.34
725	2159	52.6	33.26
750	2321	65.2	41.22
775	2507	79.3	50.11
800	2707	95.0	60.03
825	2925	113.3	71.57
850	3170	132.5	83.70

TABLE IVe. Experimental Results for Sample IL4 2-11-1

Temp. (°C)	Time (Sec.)	Weight Gain ($gm \times 10^4$)	Extent of Oxidation (Percent)
300	686	7.0	3.34
325	745	8.0	3.79
350	777	8.7	4.14
375	829	9.5	4.50
400	887	10.0	4.75
425	951	10.2	4.85
450	1014	10.5	5.01
475	1083	11.4	5.44
500	1165	12.1	5.75
525	1245	12.7	6.02
550	1339	13.8	6.56
575	1441	15.7	7.48
600	1550	19.5	9.29
625	1662	23.4	11.14
650	1739	28.8	13.71
675	1932	40.8	19.38
700	2071	53.8	25.58
725	2223	70.4	33.48
750	2393	88.3	41.99
775	2583	108.2	51.44
800	2791	132.4	62.94
825	3025	158.2	75.19
850	3299	183.1	87.03

TABLE IVf. Experimental Results for Sample IL4 5-08-1

Temp. (°C)	Time (Sec.)	Weight Gain ($gm \times 10^4$)	Extent of Oxidation (Percent)
300	641	5.4	3.43
325	682	6.0	3.77
350	727	6.3	3.98
375	780	6.8	4.27
400	830	7.0	4.42
425	890	7.1	4.48
450	955	7.1	4.50
475	1022	7.5	4.76
500	1099	7.9	4.99
525	1174	8.7	5.47
550	1267	9.7	6.12
575	1366	11.0	6.96
600	1464	12.7	8.04
625	1575	14.5	9.17
650	1702	17.2	10.88
675	1829	20.4	12.86
700	1975	25.8	16.29
725	2122	34.1	21.55
750	2287	45.6	28.81
775	2470	57.3	36.17
800	2664	70.8	44.69
825	2875	85.6	54.01
850	3127	104.3	65.82

TABLE IVg. Experimental Results for Sample IL4 5-09-1

Temp. (°C)	Time (Sec.)	Weight Gain ($gm \times 10^4$)	Extent of Oxidation (Percent)
300	648	3.4	1.87
325	694	4.0	2.15
350	742	4.7	2.55
375	790	5.1	2.75
400	842	5.6	3.04
425	902	5.9	3.20
450	967	6.3	3.44
475	1039	6.7	3.66
500	1114	7.0	3.80
525	1200	7.4	4.00
550	1286	8.2	4.45
575	1390	9.3	5.07
600	1493	11.0	5.99
625	1610	13.9	7.57
650	1728	17.7	9.63
675	1865	23.7	12.86
700	2009	32.1	17.44
725	2162	42.8	23.27
750	2335	56.4	30.65
775	2510	70.2	38.13
800	2722	85.2	46.28
825	2952	105.4	57.24
850	3206	127.0	68.97

TABLE IVh. Experimental Results for Sample IL4 4-20-2

Temp. (°C)	Time (Sec.)	Weight Gain (gm x 10^4)	Extent of Oxidation (Percent)
300	646	5.8	3.16
325	686	6.1	3.29
350	732	6.3	3.41
375	785	6.6	3.56
400	840	6.5	3.52
425	902	6.4	3.47
450	962	6.7	3.65
475	1039	7.2	3.92
500	1111	7.9	4.28
525	1169	8.8	4.75
550	1284	10.3	5.58
575	1382	11.6	6.30
600	1486	13.4	7.28
625	1603	16.0	8.69
650	1726	19.1	10.37
675	1862	23.8	12.88
700	2006	31.3	16.96
725	2155	41.7	22.62
750	2326	54.2	29.39
775	2513	67.5	36.58
800	2710	82.0	44.44
825	2938	101.5	54.99
850	3187	121.9	66.05

TABLE IVi. Experimental Results for Sample IL4 4-21-1

Temp. (°C)	Time (Sec.)	Weight Gain ($gm \times 10^4$)	Extent of Oxidation (Percent)
300	658	5.6	3.56
325	701	6.4	4.03
350	746	7.0	4.43
375	799	7.7	4.85
400	852	8.1	5.12
425	919	8.1	5.12
450	979	8.3	5.27
475	1046	8.5	5.40
500	1126	9.0	5.69
525	1215	9.6	6.05
550	1308	10.5	6.64
575	1406	11.7	7.42
600	1541	13.5	8.56
625	1637	15.7	9.95
650	1771	19.0	12.04
675	1913	23.3	14.72
700	2066	32.5	20.56
725	2232	44.2	27.99
750	2405	54.9	34.76
775	2606	68.4	43.28
800	2825	79.0	49.98
825	3082	92.7	58.63
850	3353	111.7	70.65

TABLE IVj. Experimental Results for Sample IL4 2-09-2

Temp. (°C)	Time (Sec.)	Weight Gain ($gm \times 10^4$)	Extent of Oxidation (Percent)
300	685	5.8	3.68
325	728	6.5	4.08
350	776	6.9	4.35
375	831	7.5	4.71
400	888	7.7	4.85
425	951	7.6	4.79
450	1015	7.6	4.81
475	1089	7.7	4.88
500	1167	7.9	4.98
525	1253	8.8	5.53
550	1345	9.5	5.99
575	1447	10.9	6.89
600	1555	12.5	7.90
625	1673	14.9	9.41
650	1795	18.8	11.87
675	1935	23.7	14.92
700	2082	31.6	19.92
725	2238	40.8	25.74
750	2413	52.7	33.24
775	2598	65.2	41.10
800	2808	79.3	49.99
825	3043	97.1	61.19
850	3311	115.7	72.92

TABLE IVk. Experimental Results for Sample IL4 5-06-2

Temp. (°C)	Time (Sec.)	Weight Gain ($gm \times 10^4$)	Extent of Oxidation (Percent)
300	653	4.7	2.99
325	694	5.4	3.39
350	739	5.6	3.53
375	787	6.0	3.76
400	840	6.5	4.10
425	898	6.7	4.23
450	962	6.9	4.37
475	1030	7.0	4.44
500	1109	7.2	4.54
525	1193	7.7	4.84
550	1282	8.7	5.49
575	1380	9.5	6.01
600	1483	10.8	6.83
625	1594	12.5	7.91
650	1723	15.6	9.86
675	1858	19.3	12.15
700	1995	25.5	16.09
725	2138	32.4	20.46
750	2330	41.4	26.14
775	2486	51.6	32.55
800	2698	63.4	39.99
825	2921	77.2	48.68
850	3178	93.2	58.77

TABLE IV1. Experimental Results for Sample IL4 5-07-1

Temp. (°C)	Time (Sec.)	Weight Gain ($gm \times 10^4$)	Extent of Oxidation (Percent)
300	636	5.2	2.83
325	684	5.5	2.96
350	730	5.9	3.19
375	780	6.3	3.39
400	833	6.6	3.57
425	893	6.9	3.73
450	955	7.1	3.86
475	1032	7.0	3.80
500	1104	7.6	4.11
525	1181	8.1	4.36
550	1270	9.0	4.87
575	1366	10.1	5.48
600	1469	11.7	6.35
625	1579	13.7	7.43
650	1702	17.1	9.27
675	1834	22.7	12.26
700	1970	31.4	16.98
725	2119	41.8	22.63
750	2278	54.5	29.50
775	2462	67.3	36.40
800	2662	83.0	44.89
825	2880	96.9	52.39
850	3139	113.6	61.43

TABLE IVm. Experimental Results for Sample IL4 4-19-1

Temp. (°C)	Time (Sec.)	Weight Gain ($gm \times 10^4$)	Extent of Oxidation (Percent)
300	643	6.4	3.49
325	686	6.9	3.72
350	725	7.5	4.06
375	778	7.6	4.10
400	830	7.6	4.12
425	888	7.4	4.01
450	950	7.6	4.14
475	1015	7.8	4.24
500	1092	8.0	4.33
525	1176	9.0	4.86
550	1260	10.1	5.47
575	1354	11.5	6.25
600	1452	13.1	7.12
625	1558	15.5	8.42
650	1682	18.4	9.99
675	1812	21.6	11.69
700	1949	26.9	14.57
725	2095	35.8	19.41
750	2258	48.9	26.51
775	2434	61.8	33.48
800	2614	74.0	40.09
825	2839	90.0	48.74
850	3058	106.5	57.68

TABLE IVn. Experimental Results for Sample IL4 2-08-1

Temp. (°C)	Time (Sec.)	Weight Gain ($gm \times 10^4$)	Extent of Oxidation (Percent)
300	683	5.3	3.37
325	725	5.4	3.39
350	773	5.9	3.73
375	825	6.3	3.96
400	882	6.6	4.17
425	943	6.6	4.17
450	1013	7.0	4.45
475	1081	7.1	4.51
500	1163	7.4	4.68
525	1245	7.8	4.91
550	1337	8.7	5.50
575	1437	9.5	6.03
600	1548	10.9	6.91
625	1662	13.2	8.37
650	1785	16.6	10.52
675	1913	21.5	13.57
700	2055	28.3	17.89
725	2197	38.7	24.49
750	2359	50.0	31.64
775	2541	62.0	39.20
800	2737	75.1	47.49
825	2957	89.4	56.51
850	3222	103.1	65.17

TABLE IVo. Experimental Results for Sample IL4 2-08-2

Temp. (^{o}C)	Time (Sec.)	Weight Gain (gm x 10^{4})	Extent of Oxidation (Percent)
300	678	4.6	2.20
325	720	5.1	2.41
350	767	5.3	2.52
375	818	6.1	2.88
400	871	6.7	3.18
425	930	6.7	3.18
450	996	7.0	3.34
475	1067	7.1	3.39
500	1143	7.8	3.70
525	1226	8.4	3.97
550	1313	9.2	4.37
575	1416	10.4	4.95
600	1515	12.2	5.81
625	1637	14.5	6.90
650	1752	18.8	8.94
675	1884	24.6	11.66
700	2022	34.3	16.28
725	2175	47.5	22.56
750	2340	60.8	28.88
775	2527	75.9	36.03
800	2729	92.0	43.67
825	2965	112.2	53.24
850	3219	132.3	62.79

TABLE IVp. Summary of Experimental Results

Sample	Initial Sample Weight (mg)	Particle Size	Oxidation at 850°C (%)
IL4 5-10-2	350.1	45-75 μm	79.70
IL4 4-22-2	300.0	45-75 μm	80.72
IL4 4-22-1	350.0	45-75 μm	76.45
IL4 2-10-1	300.2	45-75 μm	83.70
IL4 2-11-1	399.0	45-75 μm	87.03
IL4 5-08-1	300.6	75-150 μm	65.82
IL4 5-09-1	349.3	75-150 μm	68.97
IL4 4-20-2	350.0	75-150 μm	66.05
IL4 4-21-1	299.8	75-150 μm	70.65
IL4 2-09-2	300.9	75-150 μm	72.92
IL4 5-06-1	300.8	150-180 μm	58.77
IL4 5-07-1	350.7	150-180 μm	61.43
IL4 4-19-1	350.1	150-180 μm	57.68
IL4 2-08-1	300.0	150-180 μm	65.17
IL4 2-08-2	399.6	150-180 μm	62.79

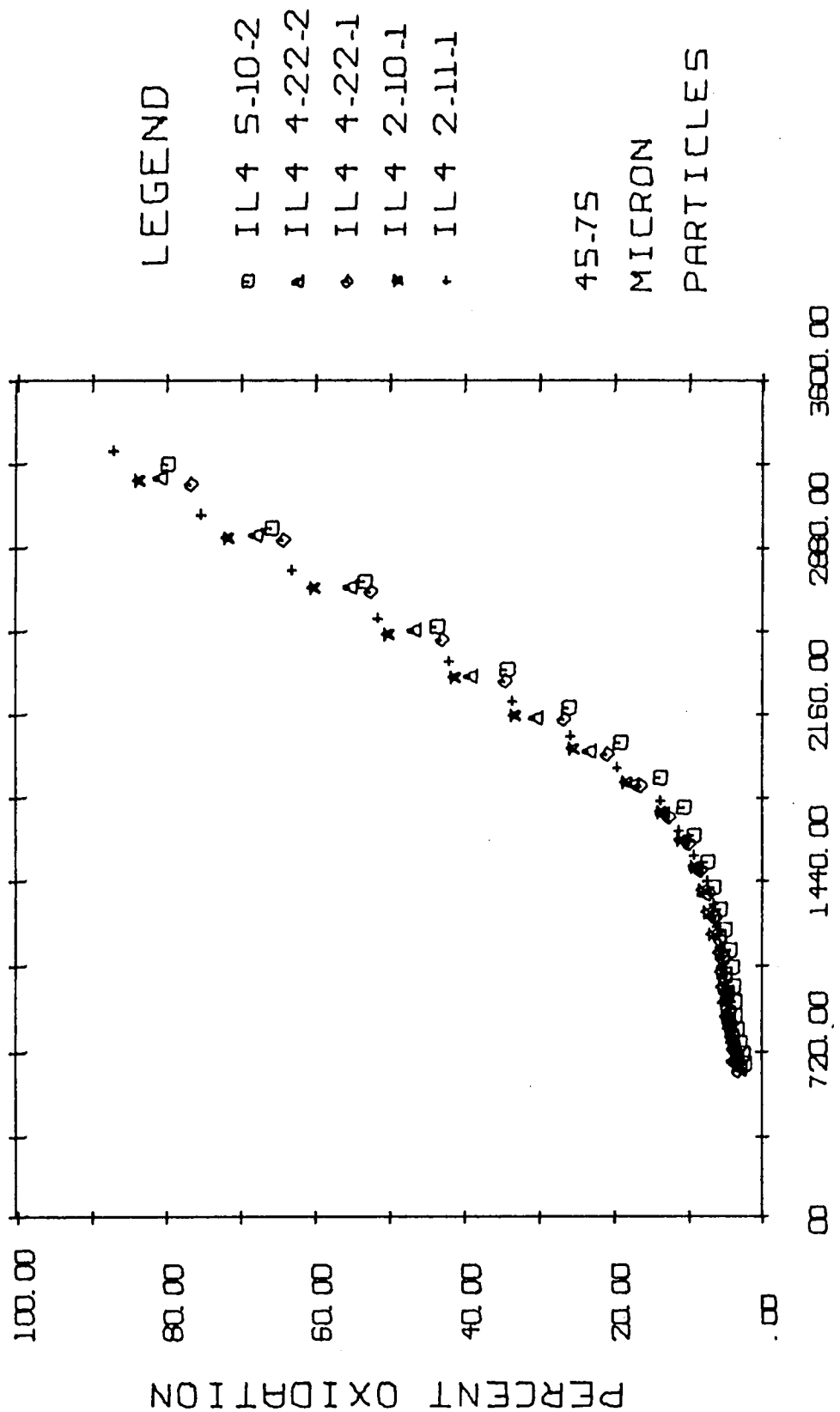

Figure 6. The percentage of theoretical oxidation versus time for the 45-75 μm particles.

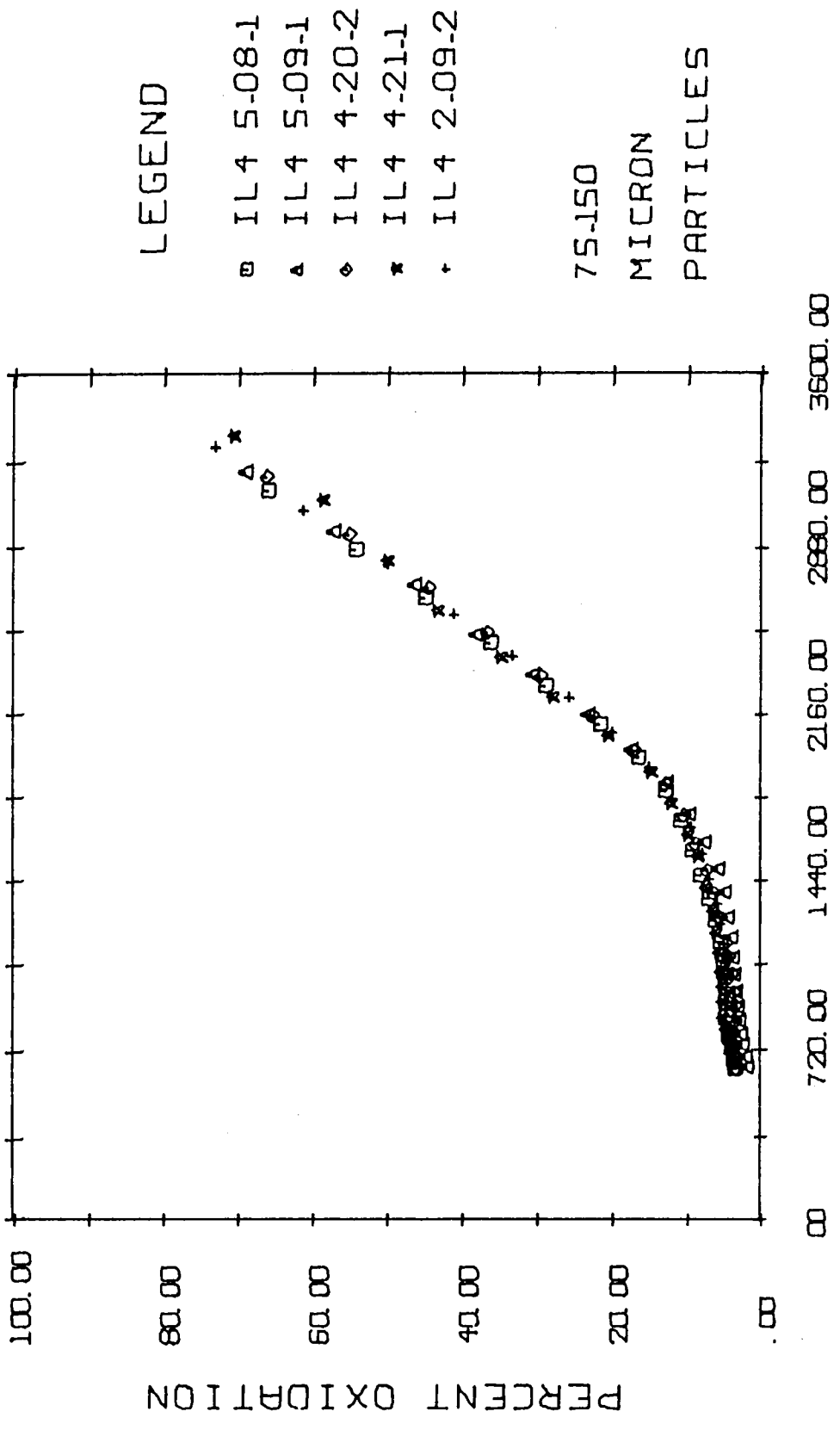

Figure 7. The percentage of theoretical oxidation versus time for 75-150 μm particles.

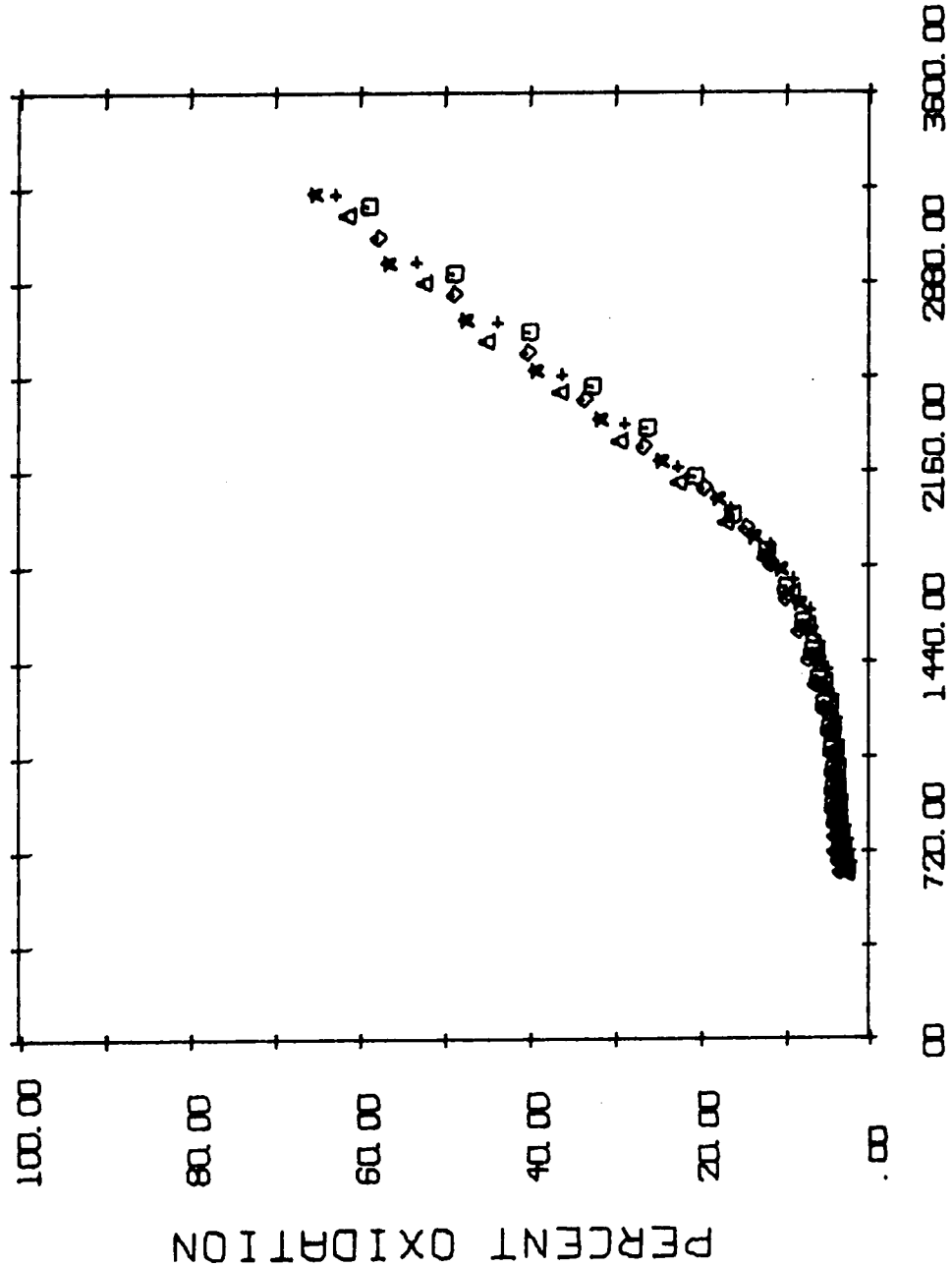

Figure 8. The percentage of theoretical oxidation versus time of 150-180 μm particles.

before the sample reached 300°C, but the stable value varied by ± 0.25 mg. The four standards were averaged together after it was shown that their behavior did not correlate with their weight.

The charts obtained from the oxidation of ilmenite were actually records of two simultaneous processes--the steady oxidation process superimposed on the somewhat erratic behavior of the standard. A ± 0.25 mg discrepancy is the same as adding or subtracting as much as ± 3 percent to the obtained results. This quantity will be taken as the upper limit of experimental error.

One outstanding feature of the graphs of oxidation is their failure to reach completion. A series of 1 gram samples were held at temperatures from 500 to 800°C for twelve hours to determine if the reaction will reach its theoretical limit of 5.27 percent weight increase. Table Va shows that at low temperatures the oxidation was very sluggish, with the process showing a pronounced particle size effect. At the higher temperatures, the specimens oxidized very rapidly, but still were not completely reacted at the end of twelve hours. Samples weighing 300 mg. were oxidized at 750°C for 24 hours (see Table Vb) with no improvement shown over the results at twelve hours. It was noted that some sintering had taken place during the longer times, especially in the very fine particles. This could explain why the smallest particles did not oxidize more thoroughly.

A major source of concern was the inability to obtain reproducible heating rates with the equipment used (Figure 9). The heating rate varied due to changes in ambient temperature. Careful consideration

TABLE Va. Weight Gained After 12 Hours at Temperature

Temperature (°C)	150-180 μm Particles		75-150 μm Particles	
	Weight Increase (Percent)	Fraction Reacted (Percent)	Weight Increase (Percent)	Fraction Reacted (Percent)
500	2.24	42.4	2.16	41.0
600	3.08	58.4	4.39	82.3
700	4.70	89.2	4.80	91.0
800	4.94	93.7	5.00	94.8

TABLE Vb. Weight Gained After 24 Hours at 750°C

Particle Size	Weight Increase (Percent)	Fraction Reacted (Percent)
45-75 μm	4.70	89.1
75-150 μm	4.76	90.4
150-180 μm	4.55	86.4

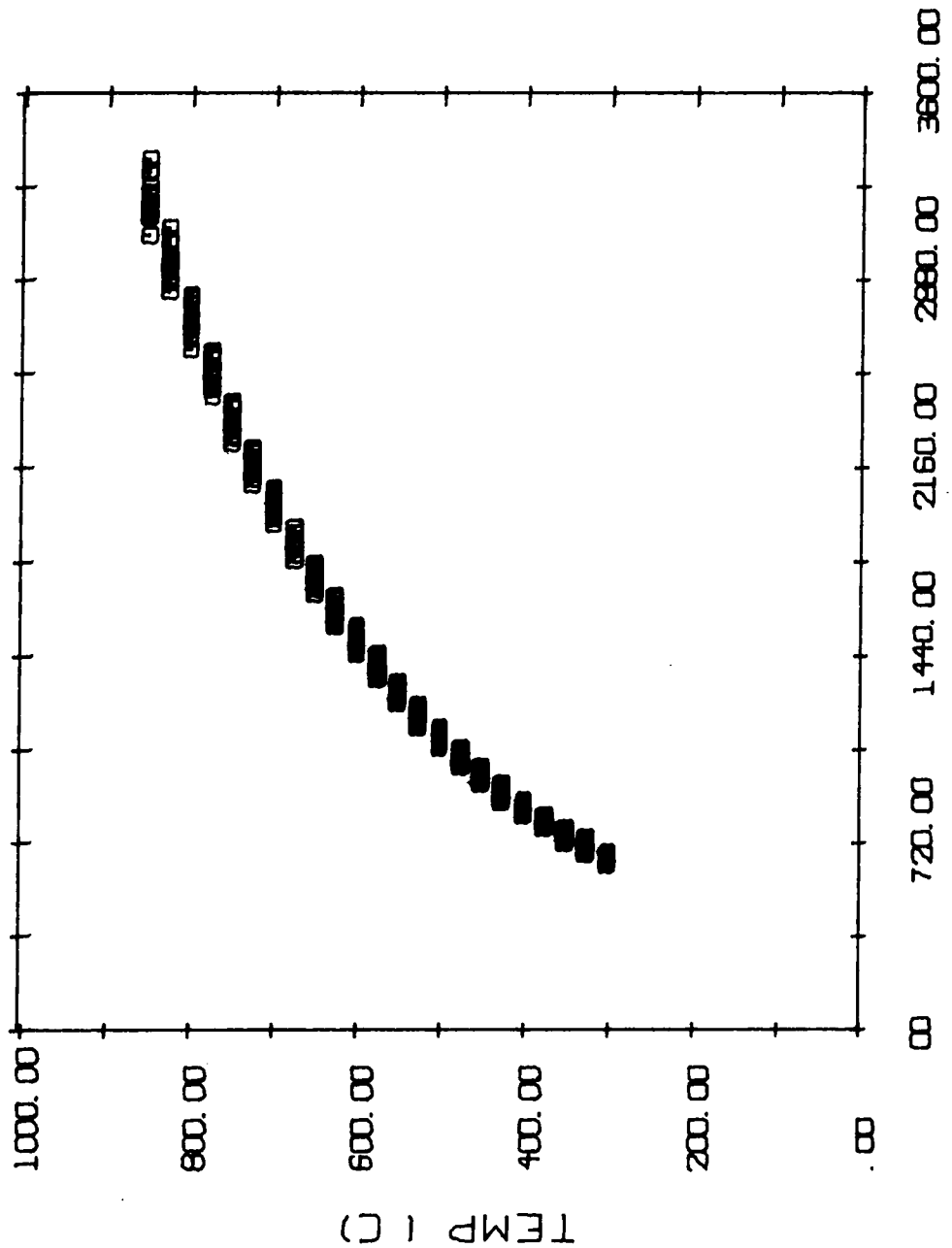

Figure 9. A plot of temperature versus time for the kinetic samples.

of the reaction process is necessary to justify the use of thermogravimetric techniques employing non-linear heating rates.

The rate of oxidation is controlled by either activation energy considerations and by the rate of supply of the reactants. These cases may be considered:

(1) if the reactants are finely interspersed, say on an atomic scale, the reaction will be controlled by the energy available. If it is less than the activation energy of the process, no reaction will occur. If it is greater, the process will occur instantaneously.

(2) If the reactants are not interspersed, as in a solid-gas reaction, and energy is available in excess of the activation energy of the process, then the rate of reaction is controlled only by the supply of any one of the reactants. Consider:

   (a) if the product forms a coherent layer on the surface of a non-porous solid, the diffusion of one of the reactants through this layer will be the rate controlling step, and the rate will be proportional to the inverse square of the product thickness.

   (b) if the product layer is not adherent to the surface, and diffusion is slow with respect to the reaction rate, the interfacial area of the shrinking particle becomes rate controlling.

For isothermal experiments, a log-log plot of $1-(1-X)^{1/3}$ versus time can be made, where X is the fractional amount of reaction that

has occurred. The slope of the plot determines the reaction mechanism. No such convenient method exists for the determination of kinetic data when the temperature is varying as the reaction occurs[33].

The method of Chatterjee[29] was first attempted, but his method was apparently not well suited to this experiment, nor was the method employed by Freeman and Carroll[28]. The reasons for this unsuitability have not been discovered. It is speculated that the major difference is in the type of sample used. When deriving their methods, both investigators employed cylindrical pellets rather than loose powder. It is not clear why this should have an effect, but results using these methods, even on "smoothed" data, were very erratic. Chatterjee's method is particularly suspect, as it requires two different sample weights. When powdered ilmenite was used, no sample height effect was demonstrated. Shah and Khalafalla[31], who employed Chaterjee's method, had cylindrical pellets whose height:diameter ratio varied from 1:1 to 1:3 as the weight was varied. The effect of this difference in geometry cannot be explained by their report. Other methods[26,27] required that a linear temperature increase be employed so that a transformation of variables could take place. These techniques obviously were not applicable.

The following method of data analysis was employed:

(1) using piecewise-linear and piecewise-polynomial curve-fitting techniques, a least squares curve was determined for each of the three size fractions (Figure 10).

Attention Patron:

Page 54 omitted from numbering

(2) the slopes of the curves were determined by numerical differentiation of the "best-fit" curve. The slope was equivalent to the reaction rate, expressed as the rate of change in the percentage of the particle that had undergone oxidation versus time.

(3) two assumptions were made at this point: (a) the particles were spherical with a diameter equal to the mean of the size distribution, and (b) the product layer formed uniformly on the surface of the sphere. Adherence of the product layer is not implied.

(4) the radius of the unreacted core of the spherical particle was calculated by:

$$r_i = [(1 - \delta_i)(r_o^3)]^{1/3}$$

where δ_i is the fractional oxidation.

(5) the thickness of the product layer, if adherent and unfractured, was calculated by

$$t_i = (r_o - r_i)(1.07)$$

This was based on a seven percent lattice expansion upon the completion of the reaction

$$4FeTiO_3 + O_2 \rightarrow 2Fe_2O_3 + 4TiO_2$$

(6) The interfacial area was based on the spherical model, and calculated by

$$a_i = 4\pi r_i^2$$

(7) the reaction mechanism would be determined from Arhenius plots of the normalized rates of reaction versus temperature. This assumes a governing relation of the form

$$R_i = R_o e^{-Q/RT_i},$$

where: R_i is the normalized rate at temperature T_i (^oK), R_o is the initial normalized rate, Q is the activation energy, R is the ideal gas constant, and T is absolute temperature.

(8) The normalization would involve nothing in the case of chemical reaction control, division by the instantaneous interfacial area if the adsorption of fluid reactants at the reaction interface is controlling, or multiplication by the square of the product thickness if diffusion is the rate determining step.

(9) Ideally, the data, if properly normalized, should fall on the same linear curve.

The data used in the making of Figures 11-13 are presented in Tables VIa-c. Inspection shows that the best agreement is obtained from Figure 13, the plot in which the reaction rate was normalized to the assumed product layer thickness. The agreement is particularly good at temperatures above 525^{o}C. The activation energies for the two sections of the curve are determined from the slope of the Arrhenius plots, as below:

$$R = R_o e^{-Q/RT}$$

Taking the logarithm of both sides, we obtain:

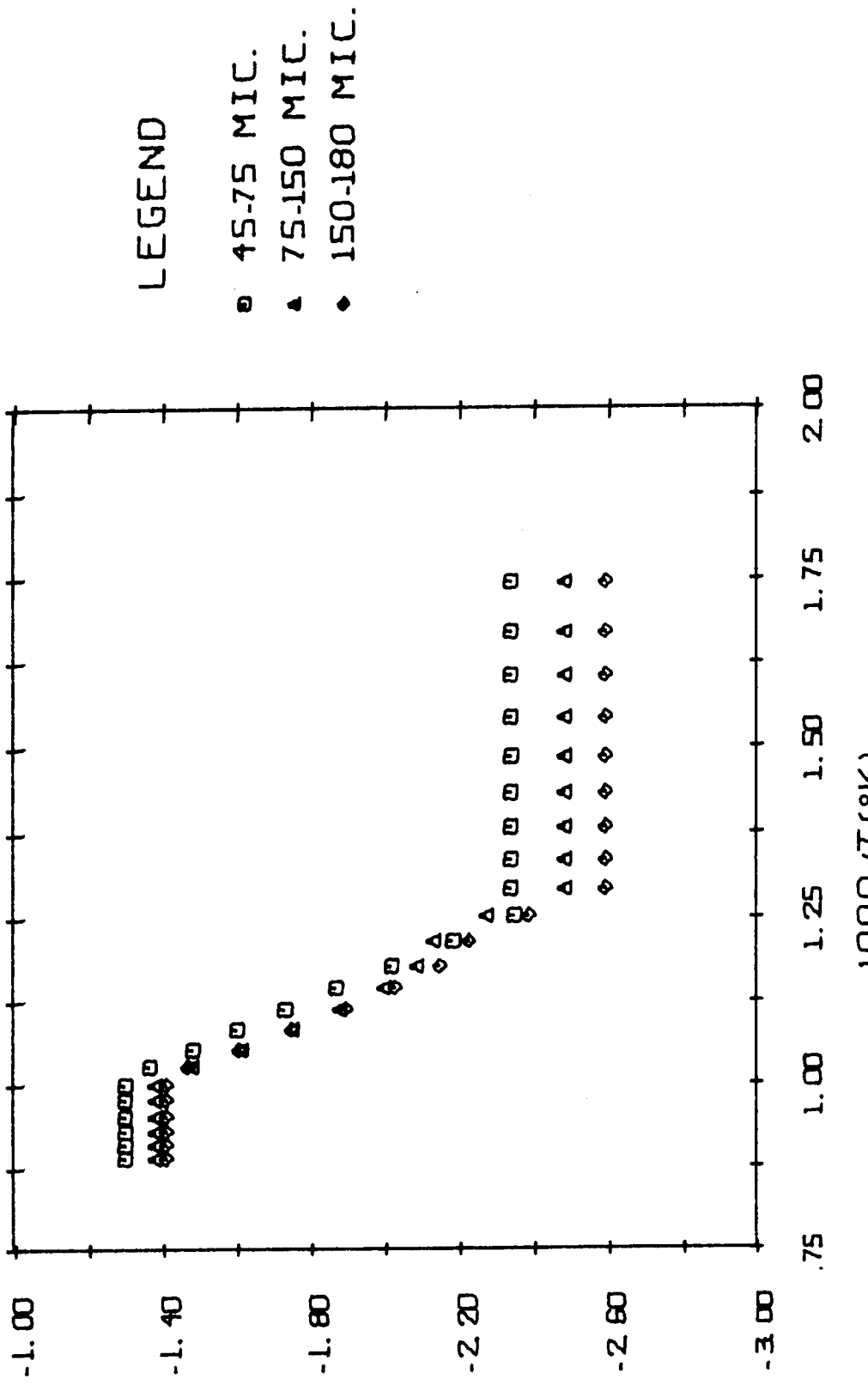

Figure 11. A plot of oxidation rate ($\log_{10}$d(% ox)/dt) versus reciprocal absolute temperature.

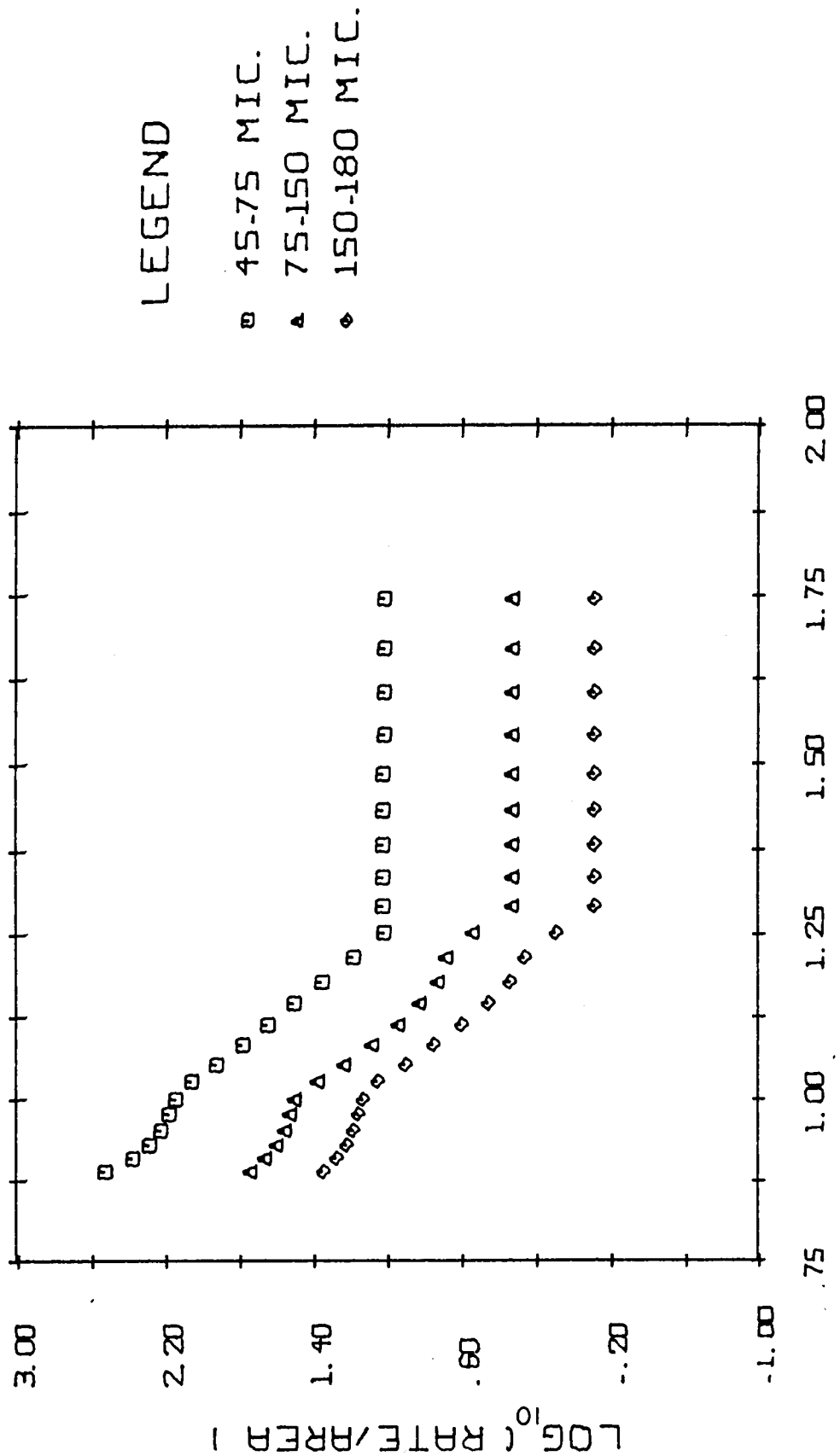

Figure 12. A plot of oxidation rate (normalized to interfacial area) versus reciprocal absolute temperature.

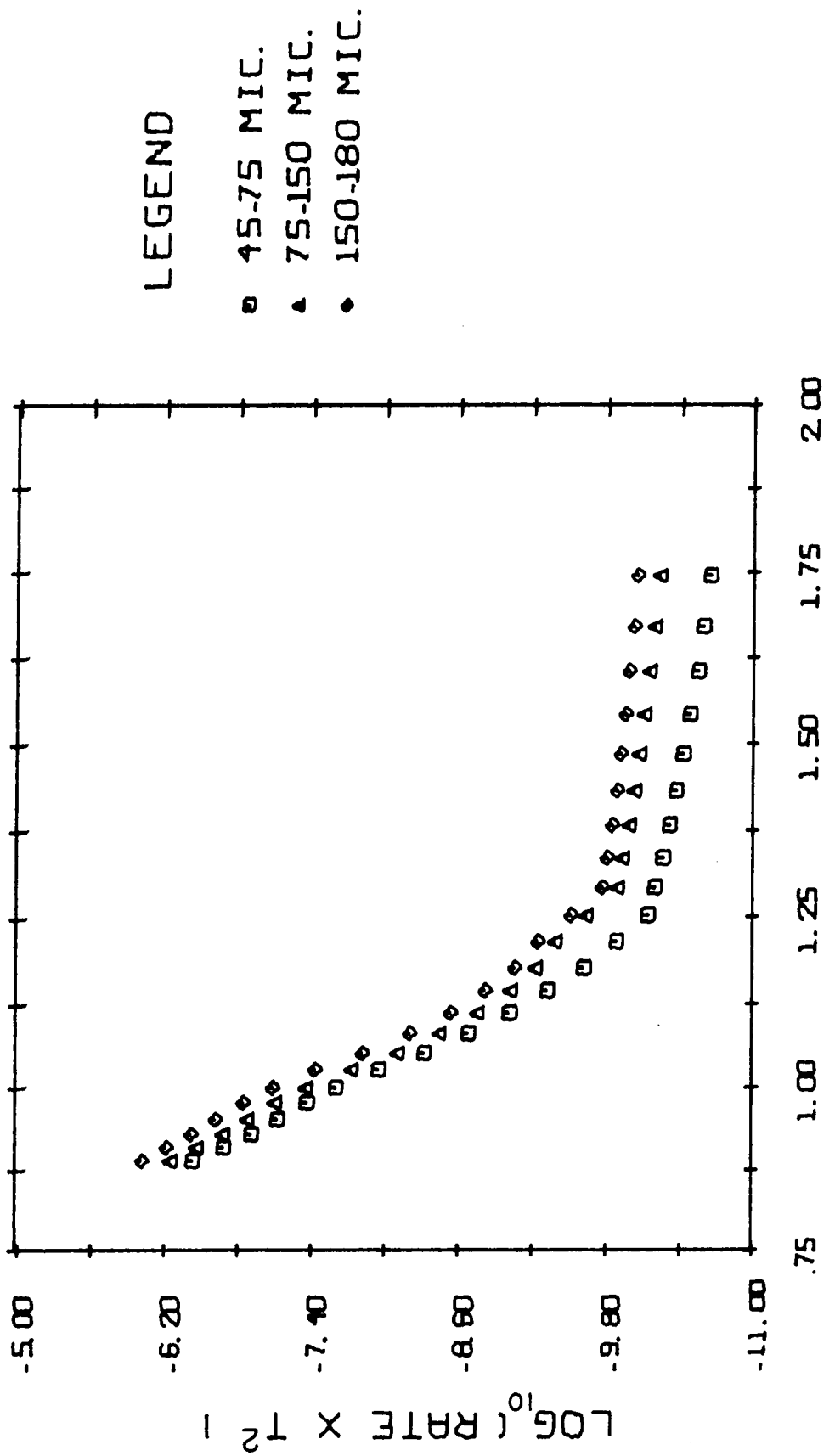

Figure 13. A plot of oxidation rate (normalized to product layer thickness squared) versus reciprocal absolute temperature.

TABLE VIa. Calculated Results for the Oxidation of 45-75 μm Particles (determined from least squares).

Temp. (°C)	Time (Sec.)	Extent of Oxidation (Percent)	Oxidation Rate (Percent/Sec.)	Interfacial Area (sq.cm.)	Product Thickness (cm.)
300	660	3.29	4.588E-03	4.424E-04	6.985E-05
325	704	3.49	4.588E-03	4.418E-04	7.421E-05
350	749	3.70	4.588E-03	4.412E-04	7.865E-05
375	801	3.94	4.588E-03	4.404E-04	8.378E-05
400	854	4.18	4.588E-03	4.397E-04	8.910E-05
425	914	4.45	4.588E-03	4.389E-04	9.497E-05
450	979	4.75	4.588E-03	4.379E-04	1.015E-04
475	1050	5.08	4.588E-03	4.369E-04	1.086E-04
500	1127	5.43	4.588E-03	4.358E-04	1.163E-04
525	1208	5.89	4.483E-03	4.345E-04	1.261E-04
550	1299	6.46	6.573E-03	4.327E-04	1.388E-04
575	1398	7.26	9.576E-03	4.302E-04	1.563E-04
600	1504	8.47	1.350E-02	4.265E-04	1.832E-04
625	1617	10.27	1.849E-02	4.208E-04	2.236E-04
650	1740	12.93	2.488E-02	4.125E-04	2.842E-04
675	1874	16.79	3.297E-02	4.002E-04	3.744E-04
700	2016	22.17	4.284E-02	3.823E-04	5.049E-04
725	2167	29.36	4.996E-02	3.588E-04	6.892E-04
750	2336	37.66	4.996E-02	3.301E-04	9.181E-04
775	2520	46.86	4.996E-02	2.968E-04	1.197E-03
800	2721	56.91	4.996E-02	2.581E-04	1.541E-03
825	2943	68.27	4.996E-02	2.105E-04	2.003E-03
850	3204	81.02	4.996E-02	1.494E-04	2.679E-03

TABLE VIb. Calculated Results for the Oxidation of 75-150 μm Particles (determined from least squares).

Temp. (°C)	Time (Sec.)	Extent of Oxidation (Percent)	Oxidation Rate Percent/Sec.)	Interfacial Area (sq.cm.)	Product Thickness (cm.)
300	660	3.36	3.305E-03	1.555E-03	1.337E-04
325	704	3.50	3.305E-03	1.553E-03	1.396E-04
350	749	3.65	3.305E-03	1.551E-03	1.456E-04
375	801	3.82	3.305E-03	1.550E-03	1.525E-04
400	854	4.00	3.305E-03	1.548E-03	1.597E-04
425	914	4.20	3.305E-03	1.546E-03	1.676E-04
450	979	4.41	3.305E-03	1.543E-03	1.764E-04
475	1050	4.65	3.305E-03	1.541E-03	1.859E-04
500	1127	4.90	3.305E-03	1.538E-03	1.963E-04
525	1208	5.16	5.351E-03	1.535E-03	2.067E-04
550	1299	5.82	7.374E-03	1.528E-03	2.336E-04
575	1398	6.58	8.204E-03	1.520E-03	2.650E-04
600	1504	7.54	1.008E-02	1.509E-03	3.047E-04
625	1617	8.84	1.319E-02	1.495E-03	3.590E-04
650	1740	10.74	1.789E-02	1.474E-03	4.390E-04
675	1874	13.57	2.457E-02	1.443E-03	5.603E-04
700	2016	17.57	3.344E-02	1.397E-03	7.413E-04
725	2167	23.50	4.186E-02	1.330E-03	1.009E-03
750	2336	30.53	4.188E-02	1.248E-03	1.351E-03
775	2520	38.24	4.188E-02	1.153E-03	1.753E-03
800	2721	46.66	4.188E-02	1.046E-03	2.233E-03
825	2948	56.19	4.188E-02	9.175E-04	2.841E-03
850	3204	66.87	4.188E-02	7.614E-04	3.639E-03

TABLE VIc. Calculated Results for the Oxidation of 150-180 μm Particles (determined from least squares).

Temp. (°C)	Time (Sec.)	Extent of Oxidation (Percent)	Oxidation Rate (Percent/Sec.)	Interfacial Area (sq.cm.)	Product Thickness (cm.)
300	660	3.16	2.559E-03	3.349E-03	1.847E-04
325	704	3.28	2.559E-03	3.346E-03	1.914E-04
350	749	3.39	2.559E-03	3.343E-03	1.982E-04
375	801	3.53	2.559E-03	3.340E-03	2.061E-04
400	854	3.66	2.559E-03	3.337E-03	2.142E-04
425	914	3.81	2.559E-03	3.334E-03	2.232E-04
450	979	3.98	2.559E-03	3.330E-03	2.331E-04
475	1050	4.16	2.559E-03	3.326E-03	2.439E-04
500	1127	4.36	2.559E-03	3.321E-03	2.556E-04
525	1208	4.62	4.087E-03	3.315E-03	2.712E-04
550	1299	5.20	5.934E-03	3.302E-03	3.056E-04
575	1398	5.84	7.111E-03	3.287E-03	3.439E-04
600	1504	6.70	9.328E-03	3.267E-03	3.959E-04
625	1617	7.94	1.278E-02	3.238E-03	4.712E-04
650	1740	9.81	1.782E-02	3.194E-03	5.859E-04
675	1874	12.64	2.482E-02	3.126E-03	7.633E-04
700	2016	16.80	3.398E-02	3.026E-03	1.030E-03
725	2167	22.85	3.861E-02	2.878E-03	1.435E-03
750	2336	29.45	3.861E-02	2.711E-03	1.902E-03
775	2520	36.56	3.861E-02	2.526E-03	2.439E-03
800	2721	44.33	3.861E-02	2.315E-03	3.073E-03
825	2948	53.11	3.861E-02	2.065E-03	3.866E-03
850	3204	62.97	3.861E-02	1.764E-03	4.883E-03

$$\ln R = \ln R_o - \left(\frac{Q}{R}\right)\frac{1}{T}$$

This shows that the slope of the Arrhenius plots should be equal to the activation energy divided by the ideal gas constant. The slopes were obtained by linear regression using the calculated data that are given in Table VII. The activation energy of the process in the initial stage (300-525°C) of reaction is 4.35 $\pm$ 0.5 kcal/mole, and is 50.2 $\pm$ 3.0 kcal/mole at higher temperatures.

In the initial stage of reaction, many features on the surface oxidize more easily than the sample as a whole. Evidence for this is two-fold: the low activation energy for the process, and the lack of a good fit to a single straight line. Diffusion control according to the assumed model does not begin until the interface begins moving uniformly toward the particle center. The activation energy obtained for the initial stage of oxidation is not generally applicable to other kinetic techniques.

Above 500°C, a very good fit to the assumed diffusion model is obtained. This fit could have been improved by a more quantitative determination of the mean particle diameters. The activation energy is of a magnitude similar to that of the diffusion process in many metals (40-60 kcal). This may be taken as confirmation of the suggestion[18] that iron is diffusing through the particle to the reaction zone.

TABLE VII. Calculated Results Used in Determination of Activation Energies by the Method of Linear Regression.

		log (Rate x Thickness^2)			
T(^{o}C)	1000/T(^{o}K)	45-75 μm Particles	75-150 μm Particles	150-180 μm Particles	Activation Energy (kcal/mole)
300	1.745	24.523	23.552	23.162	
325	1.672	24.402	23.466	23.090	
350	1.605	24.285	23.382	23.021	
375	1.543	24.159	23.289	22.942	
400	1.486	24.036	23.197	22.865	4.35 ± 0.5
425	1.433	23.908	23.100	22.783	
450	1.383	23.775	22.998	22.696	
475	1.337	23.640	22.893	22.606	
500	1.294	23.503	22.784	22.512	
525	1.253	23.364	22.199	21.965	
550	1.215	22.790	21.608	21.314	
575	1.179	22.176	21.275	20.896	
600	1.145	21.515	20.790	20.343	
625	1.114	20.802	20.193	19.680	
650	1.083	20.025	19.486	18.912	
675	1.005	19.193	18.680	18.052	
700	1.028	18.333	17.812	17.138	50.2 ± 3.0
725	1.002	17.556	16.971	16.347	
750	0.978	16.983	16.387	15.784	
775	0.954	16.452	15.866	15.287	
800	0.932	15.947	15.382	14.824	
825	0.911	15.423	14.900	14.365	
850	0.890	14.841	14.405	13.898	

CONCLUSIONS

(1) The oxidation of ilmenite has been shown to obey the following reactions:

(a) below 800°C, ilmenite oxidizes to form pseudorutile and hematite by the reaction

$$12FeTiO_3 + 3O_2 \rightarrow 4Fe_2Ti_3O_4 + 2Fe_2O_3$$

(b) above 800°C, pseudobrookite and rutile are formed according to the reaction

$$4FeTiO_3 + O_2 \rightarrow 2Fe_2TiO_5 + 2TiO_2$$

The presence of pseudorutile in a specimen heated twelve hours at 850°C indicates that it may be an intermediate compound in the reaction.

(2) The change of oxidation mechanism above 800°C should not affect an industrial process because no definite crystal structure is apparent at the end of the short periods of time needed to react finely powdered ilmenite to its apparent limit of oxidation. Also, the theoretically required amount of oxygen is unaffected by the change in reaction mechanism.

(3) The oxidation of ilmenite is diffusion controlled, with an apparent activation energy of 50 kcal/mole above 550°C. The diffusion of iron is considered to be the controlling step in this process.

(4) Thermogravimetric analysis does not require a particular variety of heating rate to give useful results. The ability to accurately model the experimental process is still the limiting factor.

(5) The rate of oxidation at 700°C is more than an order of magnitude higher than the rate at 500°C. This is an important factor in the design of any industrial process.

RECOMMENDATIONS FOR FURTHER STUDY

Of importance to any industrial process using the oxidation of ilmenite as a preliminary step is the ease with which the iron and titanium can be separated. The ferrous iron present in ilmenite is converted to ferric iron by either of the reactions shown to occur, but the oxidized ilmenite does not immediately assume any identifiable structure.

Research into the extraction of iron or titanium oxides from this 'amorphous' oxidation product should be carried out. Chemical leaching and solid state reduction are two candidates for the process.

BIBLIOGRAPHY

1. Kothari, N. C., "Recent Developments in Processing Ilmenite for Titanium", International Journal for Mineral Processing, 1, pp. 287-305 (1975).

2. Hoch, M., "Critical Review: Winning and Refining", Proceedings of the Second International Conference on Titanium Science and Technology, Vol. 1; edited by R. I. Jaffee and H. M. Burte, Plenum Press, New York, pp. 205-231 (1972).

3. Poggi, D., Charrette, G. G., and Rigaud, M., "Reducation of Ilmenite and Ilmenite Ores", Proceedings of the Second International Conference on Titanium Science and Technology, Vol. 1; edited by R. I. Jaffee and H. M. Burte; Plenum Press, New York, pp. 205-231 (1972).

4. Fetisov, V. B., Leont'ev, L. I., Kudinov, B. Z., and Ivanova, S. V., Characteristics of the Reduction of Oxidized Ilmenite Concentrates", Russian Metallurgy (Metally) 2, pp. 18-23) (1968).

5. Khairy, E. M., Hussein, M. K., and El-Tawil, S. Z., "Preoxidation of Ilmenite Ores and its Bearing on Their Solid State Reduction with Hydrogen", National Metallurgical Laboratory Technical Journal (Jamshedpur, India) 8, pp. 10-14 (1966).

6. Sinha, H. N., "Murso Process for Producing Rutile Substitutes", Proceedings of the Second International Conference on Titanium Science and Technology, Vol. 1; edited by R. I. Jaffee and H. M. Burte; Plenum Press, New York, pp. 234-245 (1972).

7. Levitskii, V. A., Popov, S. G., and Ratiani, D. D., "Thermodynamic Properties of Binary Oxide Systems at Elevated Temperatures. II. Thermodynamic Functions of Iron (II) Titanate ($FeTiO_3$) from Equilibrium and Electromotive Force Data", Russian Journal of Physical Chemistry, 45, pp. 294-296 (1971).

8. MacChesney, J. B., and Muan, A., "Studies in the System Iron Oxide-Titanium Oxide", American Mineralogist, 44, pp. 926-945 (1959).

9. Taylor, R. W., and Schmalzreid, H., "The Free Energy of Formation of Some Titanates, Silicates and Magnesium Aluminate from Measurements made with Galvanic Cells Involving Solid Electrolytes", Jorunal of Physical Chemistry, 68, pp. 2444-2449 (1964).

10. Taylor, R. W., "Phase Equilibria in the System $FeO-Fe_2O_3-TiO_2$ at 1300°C", American Mineralogist, 49, pp. 1016-1030 (1964).

11. Lindsley, D. H., "Iron-Titanium Oxides", Carnegie Institution of Washington Yearbook, 1964, pp. 144-148 (1965).

12. Akimoto, S., Nagata, T., and Katsura, T., "The $TiFe_2O_5$-Ti_2FeO_5 Solid solution Series", Nature, 179, pp. 37-38 (1957).

13. Webster, A. H., and Bright, N. F. H., "The System Iron-Titanium-Oxygen at 1200°C and Oxygen Partial Pressures between 1 Atm. and 2 x 10^{-14} Atm.", Journal of the American Ceramic Society, 44, p. 110-116 (1961).

14. Lindsley, D. H., "Investigations in the System FeO-Fe_2O_3-TiO_2", Carnegie Institution of Washington Yearbook, 1961, pp. 100-106 (1962).

15. Grieve, J., and White, J., "The System FeO-TiO_2", Journal of the Royal Technical College (Glasgow), 4, pp. 441-448 (1939).

16. MacChesney, J. B., and Maun, A., "Phase Equilibria at Liquidus Temperatures in the System Iron Oxide-Titanium Oxide at Low Oxygen Pressures", American Mineralogist, 46, pp. 572-582 (1961).

17. Rao, D. B., and Rigaud, M., "Oxidation of Ilmenite and the Product Morphology", High Temperature Science, 6, p. 323-341 (1975).

18. Temple, A. K., "Alteration of Ilmenite", Economic Geology, 61, pp. 695-714 (1966).

19. Rao, D. B., and Rigaud, M., "Kinetics of the Oxidation of Ilmenite", Oxidation of Metals, 9, pp. 99-116 (1975).

20. Grey, I. E., and Reid, A. F., "Shear Structure Compounds $(Cr,Fe)_2Ti_{n-2}O_{2n-1}$ Derived from the α-PbO_2 Structural Type", Journal of Solid State Chemistry, 4, pp. 186-194 (1972).

21. Ramdohr, P., "Important New Observations on Magnetite, Hematite, Ilmenite, and Rutile", Chemical Abstracts, 35, col. 3564 (1941).

22. Curnow, C. E., and Parry, L. G., "Oxidation Changes in Natural Ilmenite", Nature, 172, p. 1101 (1954).

23. Teufer, G., and Temple, A. K., "Pseudorutile - A New Mineral Intermediate Between Ilmenite and Rutile in the Alteration of Ilmenite", Nature, 211, pp. 179-181 (1966).

24. Overholt, J. L., Vaux, G., and Rodda, J. L., "The Nature of Arizonite", American Mineralogist, 35, pp. 117-119 (1950).

25. Karkhanalwala, M. D., and Momin, A. C., "The Alteration of Ilmenite", Economic Geology, 54, pp. 1095-1102 (1959).

26. Kubaschewski, O., and Hopkins, B. E., Oxidation of Metals and Alloys, 2nd Edition, Butterworths, London, pp. 199-201 (1962).

27. Wood, G. C., Techniques of Metals Research, Vol. 4, Physicochemical Methods in Metals Research, edited by R. A. Rapp, Part 2, Chapter 10A, "Oxidation and Corrosion", Interscience, New York, pp. 509-511 (1970).

28. Freeman, E. S., and Carroll, B., "The Application of Thermoanalytical Techniques to Reaction Kinetics. The Thermogravimetric Evaluation of the Kinetics of the Decomposition of Calcium Oxylate Monohydrate", Journal of Physical Chemistry, 62, pp. 394-397 (1958).

29. Chatterjee, P. K., "Application of Thermoanalytical Techniques to Reaction Kinetics", Journal of Polymer Science, A3, pp. 4253-4262 (1965).

30. Baur, J. P., Bridges, D. W., and Fassell, W. M., Jr., "High Pressure Oxidation of Metals: Oxidation of Metals Under Conditions of a Linear Temperature Increase", Journal of the Electrochemical Society, 102, pp. 490-496 (1955).

31. Shah, I. D., and Khalafalla, S. E., "Kinetics of Thermal Decomposition of Copper (II) Sulfate and Copper (II) Oxysulfate", U.S. Bureau of Mines Report of Investigation No. 7638 (1972).

32. Themelis, N. J., and Gauvin, W. H., "A Generalized Rate Equation for the Reduction of Iron", Transactions of the Metallurgical Society of the AIME, 227, pp. 290-300 (1963).

33. Wen, C. Y., "Noncatalytic Heterogeneous Solid-Fluid Reaction Models", Industrial and Engineering Chemistry, 60, pp. 34-54 (1968).

34. Darken, L. S., and Gurry, R. W., "The System Iron-Oxygen. I. The Wüstite Field and Related Equilibria", Journal of the American Chemical Society, 67, pp. 170-173 (1963).

35. Schwerdtfeger, K., and Turkdogan, E. T., "Techniques of Metals Research", Vol. 4, Physicochemical Methods in Metals Research, edited by R. A. Rapp, Part 1, Chapter 4, Chemical Equilibria. B. Equilibria and Transport Phenomena Involving Gas Mixtures and Condensed Phases, Interscience, New York, pp. 322-330 (1970).

36. Bailey, S. W. Cameron, E. N., Spedden, H. R., and Weege, R. J."The Alteration of Ilmenite in Beach Sands", Economic Geology, 51, pp. 263-279 (1956).

The vita has been removed from the scanned document

THE OXIDATION OF ILMENITE: A KINETIC STUDY

by

Lawrence J. Corsa, III

(ABSTRACT)

Synthetically obtained ilmenite ($FeO \cdot TiO_2$) particles were oxidized under conditions of a non-linear temperature increase over the range 300°-$850^{\circ}C$. Short-circuit diffusion in the initial stages of oxidation gave an activation energy of 4.35 ± 0.4 kcal/mole, while above $525^{\circ}C$ the activation energy was 50.2 ± 3.0 kcal/mole. The process was shown to be diffusion controlled, with iron the likely mobile species above $525^{\circ}C$, while no mechanism could be singled out for the controlling step in the early stages.

The oxidation products in O_2 after 24 hours were shown to be pseudorutile ($Fe_2Ti_3O_9$) and hematite (Fe_2O_3) in a finely dispersed phase at temperatures below about $800^{\circ}C$, with pseudobrookite (Fe_2TiO_5) and rutile (TiO_2) being stable above this temperature.